Kalman Filters in Non-uniformly Sampled Multirate Systems: for FDI and Beyond

Weihua Li[+], Sirish L. Shah[+,*], Deyun Xiao[§]
[+] Department of Chemical and Materials Engineering,
University of Alberta, Edmonton, Alberta, T6G 2G6, Canada
[§] Department of Automation, Tsinghua University, Beijing, 100084, China

February 23, 2006

Abstract

This paper consists of two parts. The first part is the development of a data-driven Kalman filter for a non-uniformly sampled multirate (NUSM) system, including identification of the state space model and estimation of noise covariance matrices of the NUSM system. Algorithms for both one-step prediction and filtering are developed, and analysis of stability and convergence is conducted in the NUSM framework. The second part of the paper investigates a Kalman filter-based methodology for unified detection and isolation of sensor, actuator, and process faults in the NUSM system with analysis on fault detectability and isolability. Case studies using data collected from a pilot scale experimental plant and numerical examples are provided to justify the practicality of the proposed theory.

Keywords: non-uniformly sampled multirate systems, Kalman filters, one-step prediction, filtering, unified fault detection and isolation

1 Introduction

Since the publication of Kalman's landmark paper (Kalman, 1960), Kalman filters have become ubiquitous in state estimation, system identification, adaptive control, signal processing and have found many industrial applications (Sorenson, 1970, 1985; Haykin, 1996). In a chemical engineering process, Kalman filters are frequently used either to estimate unmeasurable process variables based on available measurements of other process variables or to

*Corresponding author. Phone: 1-780-492-5162. Email: sirish.shah@ualberta.ca

filter the measured process variables if they are noisy. There exist Kalman filtering algorithms for continuous-time (CT) systems and discrete-time (DT) systems (Sorenson, 1985). However, most of the DT algorithms are for single rate systems only.

In many industrial processes, variables are sampled at more than one rate, i.e. *multiple rates*. Take a polymer reactor as an example, where the manipulated variables can be adjusted at relatively fast rates (Gudi et al., 1994), while the measurements of quality variables, e.g. the composition and density, are typically obtained after several minutes of analysis. Furthermore, the sampling is termed as *non-uniform*, if the sampling intervals for each variable are *non-equally* spaced, as is typically the case when manual samples are taken for laboratory analysis.

First, this paper attempts to develop the Kalman filter for a NUSM system, including algorithms for one step prediction and filtering. The development is conducted in a generic framework: where each variable in a physical system is sampled at non-uniform rates. Non-uniform sampling has other advantages over uniform sampling, such as always preserving controllability and observability (uniform sampling only preserves them conditionally) in discretization, as pointed out by Sheng et.al (2002).

Suppose that one describes a NUSM system by a *lifted* state space model, e.g. $\{\underline{\mathbf{A}}, \underline{\mathbf{B}}, \underline{\mathbf{C}}, \underline{\mathbf{D}}\}$. In the development of the Kalman filter, no knowledge regarding the state space model and the covariance matrices of process and measurement noise in the NUSM system is assumed. Alternatively, a subspace method of identification (SMI) for $\{\underline{\mathbf{A}}, \underline{\mathbf{B}}, \underline{\mathbf{C}}, \underline{\mathbf{D}}\}$ and the covariances is proposed; such a SMI is a component of the data-driven Kalman filter.

The second part of this paper is concerned with the development of a novel Kalman filter-based approach towards unified detection and isolation of sensor, actuator, and process faults in NUSM systems. For single rate systems, Mehra and Peschon were the pioneers in applying Kalman filters for fault detection (Mehra and Peschon, 1971). Kalman filter-based fault detection and isolation (FDI) methods proposed before the 1990s have been surveyed by Willsky (1976) and Frank (1990). Most recently, Keller's work (Keller, 1999) represented the state of art in this area. The common feature of the above-mentioned FDI schemes is that they are applicable only for actuator and process faults and have difficulty in isolating

sensor faults, as analyzed by White and Speyer (1984).

Recently, FDI in multirate systems has significant attracted research attention. Fadali and Liu (1998), Fadali and Shabaik (2002), and Zhang et al. (2002) have considered FDI issues in uniformly sampled multirate systems. Furthermore, Li and Shah (2004) and Li et al. (2006) have developed detection and isolation methodology for sensor and actuator faults in NUSM systems. This paper investigates a novel Kalman filter-based FDI scheme that works for detection and isolation of faults in actuators, sensors, and process components in NUSM systems. The relevant analysis on fault detectability and isolability is also given.

This paper is organized as follows. The problem is formulated in Section 2, where the lifted model of a NUSM system in the fault-free case is introduced. Section 3 is mainly devoted to the development of a SMI for NUSM systems. Note that the SMI developed in this paper is different from that in Li et al. (2006). While the former identifies the system matrices and covariance matrices of noise and disturbance in a NUSM system, the latter identifies the Chow-Willsky approach-based residual model for fault detection. A complete set of Kalman filter algorithms, including one-step prediction and filtering algorithms, are developed in Section 4. Therein, convergence and stability analysis of the algorithms is also performed. A novel Kalman filter-based approach towards unified detection and isolation of sensor, actuator, and process faults in the NUSM system is investigated in Section 5. The developed FDI scheme is applied to a pilot scale experimental plant in Section 6, where a successful case study on actuator and sensor FDI has been conducted. Moreover, a numerical example to show the power of Kalman filter on filtering is also provided. The paper ends with concluding remarks in Section 7. Detailed derivation of an equation is documented in the Appendix.

2 Problem formulation

Consider a multi-input multi-output (MIMO) system represented by the following CT state space model:

$$\dot{\mathbf{x}}(t) = \mathbf{A}\mathbf{x}(t) + \mathbf{B}\tilde{\mathbf{u}}(t) + \boldsymbol{\phi}(t), \quad \tilde{\mathbf{y}}(t) = \mathbf{C}\mathbf{x}(t) + \mathbf{D}\tilde{\mathbf{u}}(t) \tag{1}$$

where (i) $\tilde{\mathbf{u}}(t) \in \Re^l$ and $\tilde{\mathbf{y}}(t) \in \Re^m$ are *noise-free* inputs and outputs, respectively; (ii) $\mathbf{x}(t) \in \Re^n$ is the state; (iii) $\boldsymbol{\phi}(t) \in \Re^n$ is the disturbance vector assumed to be a stationary Gaussian white noise vector with covariance $\mathbf{R}_\phi \in \Re^{n \times n}$, i.e. $\boldsymbol{\phi}(t) \sim \aleph(\mathbf{0}, \mathbf{R}_\phi)$; and (iv) $\mathbf{A}$, $\mathbf{B}$, $\mathbf{C}$ and $\mathbf{D}$ are unknown system matrices with compatible dimensions. In the sequel throughout the paper, the notation, $\aleph(\mathbf{0}, \mathbf{R})$, is used to stand for a Gaussian white noise vector with covariance $\mathbf{R}$. It is further assumed that (i) the pair $(\mathbf{A}, \mathbf{C})$ is observable, (ii) the pair $(\mathbf{A}, \mathbf{B}\mathbf{R}_\phi^{1/2})$ is controllable, and (iii) the stochastic part of $\mathbf{A}$ is asymptotically stable (Van Overschee and De Moor, 1996).

The following non-uniformly multirate sampling approach as depicted in Figure 1 is employed to collect measurements from the system described by Eqn. 1. More specifically, for

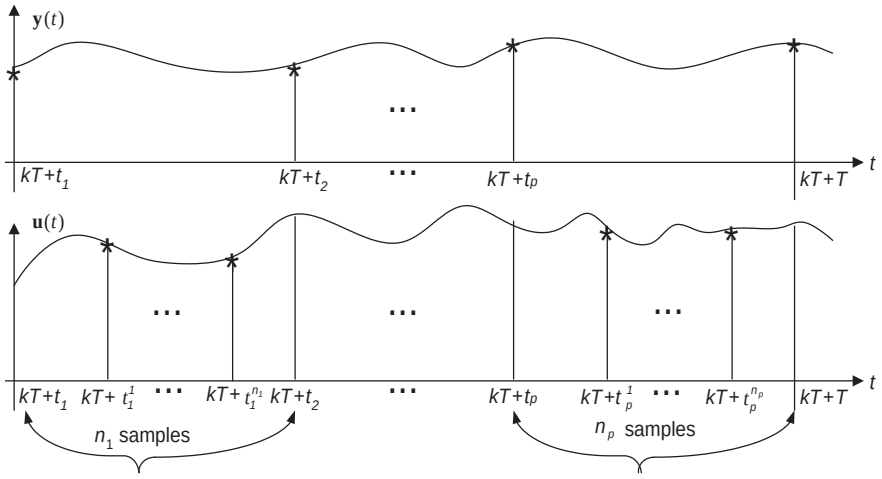

Figure 1: *Non-uniform and multirate sampling of the inputs and outputs*

a given *frame period*, T, over the k^{th} frame period $[kT, kT+T)$, the inputs and outputs are sampled as follows.

- An output variable is sampled p times at time instants: $\{kT+t_1, kT+t_2, \cdots, kT+t_p\}$, where $0 = t_1 < t_2 < \cdots < t_p < T$.

- An input variable is sampled g times. Moreover, within the time interval $[kT+t_i, kT+t_{i+1})$, for $i \in [1, p]$, n_i samples of the input variable are taken at time instants: $\{kT+t_i^1, kT+t_i^2, \cdots, kT+t_i^{n_i}\}$, where $t_i \leq t_i^1 < t_i^2 \cdots < t_i^{n_i} < t_{i+1}$ and $t_{p+1} = T$. Note that

theoretically, $n_i \geq 0$ and $g = n_1 + n_2 + \cdots + n_p$ can be larger/less than, or equal to p. However, in engineering practice, usually $g \geq p$, i.e. in general fewer samples of outputs than inputs are available.

The sampling is repeated over the next frame period.

In the most general case, each of the inputs, outputs, and disturbances can be sampled differently. However, for simplicity of mathematical manipulation and without loss of generality it is assumed that (i) the l inputs, $\tilde{\mathbf{u}}(t)$, and the n disturbances, $\boldsymbol{\phi}(t)$, are sampled at one rate; and (ii) the m outputs, $\tilde{\mathbf{y}}(t)$, are sampled at a slower common rate. Accordingly, the lifted vectors for inputs and outputs are constructed as follows, respectively,

$$\begin{aligned} \underline{\tilde{\mathbf{u}}}(k) &= \left[\ \tilde{\mathbf{u}}'(kT+t_1^1)\cdots\tilde{\mathbf{u}}'(kT+t_1^{n_1})\cdots\tilde{\mathbf{u}}'(kT+t_p^1)\cdots\tilde{\mathbf{u}}'(kT+t_p^{n_p})\ \right]' \in \Re^{lg} \\ \underline{\tilde{\mathbf{y}}}(k) &= \left[\ \tilde{\mathbf{y}}'(kT+t_1)\cdots\tilde{\mathbf{y}}'(kT+t_p)\ \right]' \in \Re^{mp}, \end{aligned} \tag{2}$$

where $'$ represents the transpose of the argument. In addition, the lifted vector for the disturbance, $\underline{\boldsymbol{\phi}}(k) \in \Re^{ng}$, is structurally identical to $\underline{\tilde{\mathbf{u}}}(k)$.

At the time instant $kT + t_i$, for $i \in [1, p]$, the sampled outputs are

$$\mathbf{y}(kT+t_i) = \tilde{\mathbf{y}}(kT+t_i) + \mathbf{o}(kT+t_i) \in \Re^m \tag{3}$$

where $\mathbf{o}(\ ) \sim \aleph(\mathbf{0}, \mathbf{R}_o)$ is the measurement error and independent of the initial state, $\mathbf{x}(0)$. However, at instant $kT + t_i^j$ for $i \in [1, p]$ and $j \in [1, n_i]$, assume that $\tilde{\mathbf{u}}(kT + t_i^j)$ be available, i.e. $\mathbf{u}(kT + t_i^j) = \tilde{\mathbf{u}}(kT + t_i^j)$. They are outputs of controllers and are known in a closed-loop system when one ignores the noise in the actuators.

It follows from Eqn. 3 that $\underline{\mathbf{y}}(k) = \underline{\tilde{\mathbf{y}}}(k) + \underline{\mathbf{o}}(k) \in \Re^{mp}$, where $\underline{\mathbf{y}}(k)$ (or $\underline{\mathbf{o}}(k)$) has an identical structure to $\underline{\tilde{\mathbf{y}}}(k)$. Besides, $\underline{\mathbf{o}}(k) \sim \aleph(\mathbf{0}, \underline{\mathbf{R}}_o)$ with $\underline{\mathbf{R}}_o = \mathbf{I}_p \otimes \mathbf{R}_o \in \Re^{mp \times mp}$, where $\otimes$ is the Kronecker tensor product and $\mathbf{I}_l$ denotes an $l \times l$ identity matrix. In the sequel, any $\kappa \times \kappa$ identity matrix is denoted by $\mathbf{I}_\kappa$. As derived in the Appendix, the lifted model of Eqn. 1 is as follows:

$$\mathbf{x}(k+1) = \underline{\mathbf{A}}\ \mathbf{x}(k) + \underline{\mathbf{B}}\ \underline{\mathbf{u}}(k) + \underline{\mathbf{W}}\ \underline{\boldsymbol{\phi}}(k), \quad \underline{\mathbf{y}}(k) = \underline{\mathbf{C}}\ \mathbf{x}(k) + \underline{\mathbf{D}}\ \underline{\mathbf{u}}(k) + \underline{\mathbf{J}}\ \underline{\boldsymbol{\phi}}(k) + \underline{\mathbf{o}}(k) \tag{4}$$

where (i) $\underline{\mathbf{A}}$, $\underline{\mathbf{B}}$, $\underline{\mathbf{C}}$, $\underline{\mathbf{D}}$, $\underline{\mathbf{J}}$, and $\underline{\mathbf{W}}$ are functions of $\mathbf{A}$, $\mathbf{B}$, $\mathbf{C}$, $\mathbf{D}$, t_i, and $t_i^{n_i}$, $\forall\ i \in [1, p]$; (ii) $\underline{\boldsymbol{\phi}}(k) \sim \aleph(\mathbf{0}, \underline{\mathbf{R}}_\phi)$ with $\underline{\mathbf{R}}_\phi = \mathbf{I}_n \otimes \mathbf{R}_\phi \in \Re^{ng \times ng}$.

It is assumed that the frame period T is non-pathological relative to matrix $\mathbf{A}$. As a consequence, Eqn. 4 does preserve the causality, controllability and observability of Eqn. 1 in line with the analysis of Sheng et al. (2002). Define $\underline{\boldsymbol{\omega}}(k) \equiv \underline{\mathbf{W}}\ \underline{\boldsymbol{\phi}}(k) \in \Re^n$ and $\underline{\boldsymbol{\varepsilon}}(k) \equiv \underline{\mathbf{J}}\ \underline{\boldsymbol{\phi}}(k) + \underline{\mathbf{o}}(k) \in \Re^{mp}$, which are stationary Gaussian white noise vectors with the following auto/cross-covariances: $\underline{\mathbf{R}}_{\omega} = E\{\underline{\boldsymbol{\omega}}(k)\underline{\boldsymbol{\omega}}'(k)\} = \underline{\mathbf{W}}\ \underline{\mathbf{R}}_{\phi}\underline{\mathbf{W}}' \in \Re^{n\times n}$, $\underline{\mathbf{R}}_{\varepsilon} = E\{\underline{\boldsymbol{\varepsilon}}(k)\underline{\boldsymbol{\varepsilon}}'(k)\} = \underline{\mathbf{J}}\ \underline{\mathbf{R}}_{\phi}\underline{\mathbf{J}}' + \underline{\mathbf{R}}_{o} \in \Re^{mp\times mp}$, $\underline{\mathbf{R}}_{\omega,\varepsilon} = E\{\underline{\boldsymbol{\omega}}(k)\underline{\boldsymbol{\varepsilon}}'(k)\} = \underline{\mathbf{W}}\ \underline{\mathbf{R}}_{\phi}\underline{\mathbf{J}}' \in \Re^{n\times mp}$. Note that $E(\ )$ stands for the expectation operator. Eqn. 4 can be rewritten as:

$$\mathbf{x}(k+1) = \underline{\mathbf{A}}\ \mathbf{x}(k) + \underline{\mathbf{B}}\ \underline{\mathbf{u}}(k) + \underline{\boldsymbol{\omega}}(k), \quad \underline{\mathbf{y}}(k) = \underline{\mathbf{C}}\ \mathbf{x}(k) + \underline{\mathbf{D}}\ \underline{\mathbf{u}}(k) + \underline{\boldsymbol{\varepsilon}}(k) \tag{5}$$

Eqn. 5 is the lifted model of a NUSM system. This paper first considers the following problems:

- Given data: $\{\underline{\mathbf{u}}(1), \underline{\mathbf{y}}(1), \underline{\mathbf{u}}(2), \underline{\mathbf{y}}(2), \cdots, \underline{\mathbf{u}}(N), \underline{\mathbf{y}}(N)\}$, as $N \to \infty$, develop a SMI that identifies the system matrices, $\{\underline{\mathbf{A}}, \underline{\mathbf{B}}, \underline{\mathbf{C}}, \underline{\mathbf{D}}\}$, and estimates the covariance matrices, $\underline{\mathbf{R}}_{\epsilon}$, $\underline{\mathbf{R}}_{\omega}$, $\underline{\mathbf{R}}_{\omega,\varepsilon}$, consistently;

- Develop the Kalman filter, including the one-step prediction and filtering algorithms, for Eqn. 5.

Later in Section 5, we investigate a Kalman filter-based methodology for unified detection and isolation of actuators, sensors, and process faults in the NUSM system.

3 Subspace Identification of the NUSM System

Since the late 1980s, due to their appealing numerical properties for systems with high dimensionality, the SMI algorithms have been successfully applied to multivariate DT single rate systems (Moonen et al., 1989; Verhaegen and Dewilde 1992a, 1992b; Van Oveschee and De Moor, 1994). Recently, SMI algorithms for uniformly sampled multirate systems (Li et al., 2001), and NUSM systems for residual models to perform FDI (Li et al., 2006) have been reported. This paper proposes an SMI, which will have a more generic applicability in contrast to the existing work, for the system described by Eqn. 5.

With $i > n$, $\underline{\mathbf{\Gamma}}_1 = \underline{\mathbf{C}}$, and $\underline{\mathbf{H}}_1 = \underline{\mathbf{D}}$, define

$$\underline{\mathbf{\Gamma}}_i \equiv \begin{bmatrix} \underline{\mathbf{C}} \\ \underline{\mathbf{\Gamma}}_{i-1}\underline{\mathbf{A}} \end{bmatrix} \in \Re^{imp \times n} \text{ and } \underline{\mathbf{H}}_i \equiv \begin{bmatrix} \underline{\mathbf{D}} & \mathbf{0} \\ \underline{\mathbf{\Gamma}}_{i-1}\underline{\mathbf{B}} & \underline{\mathbf{H}}_{i-1} \end{bmatrix} \in \Re^{imp \times igl}.$$

Since the pair $(\underline{\mathbf{C}}, \underline{\mathbf{A}})$ is observable, $\underline{\mathbf{\Gamma}}_i$ has rank n. Define a stacked vector, $\underline{\boldsymbol{\xi}}_i(k) = \begin{bmatrix} \underline{\boldsymbol{\xi}}'(k) & \cdots & \underline{\boldsymbol{\xi}}'(k+i-1) \end{bmatrix}'$, where $\underline{\boldsymbol{\xi}}(k)$ can be $\underline{\mathbf{u}}(k)$ or $\underline{\mathbf{y}}(k)$. Using stacked vectors, we form block Hankel matrices,

$$\underline{\mathbf{U}}_{0,i-1} = [\underline{\mathbf{u}}_i(0) \ \cdots \ \underline{\mathbf{u}}_i(N-1)] = \begin{bmatrix} \underline{\mathbf{u}}(0) & \underline{\mathbf{u}}(1) & \cdots & \underline{\mathbf{u}}(N-1) \\ \underline{\mathbf{u}}(1) & \underline{\mathbf{u}}(2) & \cdots & \underline{\mathbf{u}}(N) \\ \vdots & \vdots & \vdots & \vdots \\ \underline{\mathbf{u}}(i-1) & \underline{\mathbf{u}}(i) & \cdots & \underline{\mathbf{u}}(i+N-2) \end{bmatrix} \in \Re^{ilg \times N}$$

and $\underline{\mathbf{Y}}_{0,i-1} = \underline{\mathbf{U}}_{0,i-1}|_{\underline{\mathbf{u}}(\ )=\underline{\mathbf{y}}(\ )} \in \Re^{imp \times N}$, where $N \to \infty$; the subscripts, "$0''$ and "$i-1''$, indicate the time stamps of the $(1,1)$ and $(i,1)$ block elements of a matrix.

For two compatible matrices, $\mathbf{A}_1$ and $\mathbf{A}_2$, we define

$$\mathbf{A}_1/\mathbf{A}_2 \equiv \mathbf{A}_1\mathbf{A}_2'\left(\mathbf{A}_2\mathbf{A}_2'\right)^{-1}\mathbf{A}_2 \tag{6}$$

as the projection of $\mathbf{A}_1$ onto the row space of $\mathbf{A}_2$. Such a projection is the optimal prediction of $\mathbf{A}_1$ based on $\mathbf{A}_2$ in the sense that the squared Frobenius norm, $\|\mathbf{A}_1 - \mathbf{A}_2\|_F^2$, is minimized subject to: row space of $\mathbf{A}_1 \subset$ row space of $\mathbf{A}_2$. Applying Eqn. 6, we define

$$\underline{\mathbf{Z}}_i = \underline{\mathbf{Y}}_{i,2i-1} / \begin{bmatrix} \underline{\mathbf{U}}_{0,i-1} \\ \underline{\mathbf{U}}_{i,2i-1} \\ \underline{\mathbf{Y}}_{0,i-1} \end{bmatrix} \in \Re^{imp \times N} \text{ and } \underline{\mathbf{Z}}_{i+1} = \underline{\mathbf{Y}}_{i+1,2i-1} / \begin{bmatrix} \underline{\mathbf{U}}_{0,i-1} \\ \underline{\mathbf{U}}_{i+1,2i-1} \\ \underline{\mathbf{Y}}_{0,i} \end{bmatrix} \in \Re^{(i-1)mp \times N},$$

where $\underline{\mathbf{Z}}_i$ is the optimal prediction of $\underline{\mathbf{Y}}_{i,2i-1}$ given $\underline{\mathbf{U}}_{0,i-1}$, $\underline{\mathbf{U}}_{i,2i-1}$, $\underline{\mathbf{Y}}_{0,i-1}$; $\underline{\mathbf{Z}}_{i+1}$ is similar to $\underline{\mathbf{Z}}_i$; $\underline{\mathbf{Y}}_{i,2i-1}/\underline{\mathbf{Y}}_{i+1,2i-1}$ and $\underline{\mathbf{U}}_{i,2i-1}/\underline{\mathbf{U}}_{i+1,2i-1}$ are analogous to $\underline{\mathbf{Y}}_{0,i-1}$ and $\underline{\mathbf{U}}_{0,i-1}$, respectively.

The detailed derivation and consistency analysis of the SMI algorithm for Eqn. 5 is similar to those of the N4SID (Van Overschee and De Moor, 1994). We give the main results of the algorithm as follows:

- Using Eqn. 6, calculate $\underline{\mathbf{Z}}_i = [\mathbf{L}_i^1|\ \mathbf{L}_i^2|\ \mathbf{L}_i^3] \begin{bmatrix} \underline{\mathbf{U}}_{0,i-1}' & \underline{\mathbf{U}}_{i,2i-1}' & \underline{\mathbf{Y}}_{0,i-1}' \end{bmatrix}'$ and

$$\underline{\mathbf{Z}}_{i+1} = \left[\mathbf{L}_{i+1}^1|\ \mathbf{L}_{i+1}^2|\ \mathbf{L}_{i+1}^3\right] \begin{bmatrix} \underline{\mathbf{U}}_{0,i}' & \underline{\mathbf{U}}_{i+1,2i-1}' & \underline{\mathbf{Y}}_{0,i}' \end{bmatrix}'.$$

- Calculate the singular value decomposition: $[\mathbf{L}_i^1|\ \mathbf{L}_i^3]\left[\begin{array}{cc}\underline{\mathbf{U}}'_{0,i-1} & \underline{\mathbf{Y}}'_{0,i-1}\end{array}\right]' = \mathbf{U}_1\mathbf{\Lambda}_1\mathbf{V}_1'$, where $\mathbf{\Lambda}_1$ is a diagonal matrix containing the non-zero singular values, and $\mathbf{U}_1$ and $\mathbf{V}_1$ are the associated left and right singular vectors, respectively. The order, n, is equal to the number of non-zero singular values. Select $\underline{\mathbf{\Gamma}}_i = \mathbf{U}_1\mathbf{\Lambda}_1^{1/2}$ (up to a column space).

- Determining the least squares solution:

$$\left[\begin{array}{c}\underline{\mathbf{\Gamma}}_{i-1}^+\underline{\mathbf{Z}}_{i+1}\\ \underline{\mathbf{Y}}_{i,i}\end{array}\right] = \left[\begin{array}{cc}\mathbf{K}_1 & \mathbf{K}_2\end{array}\right]\left[\begin{array}{c}\underline{\mathbf{\Gamma}}_i^+\underline{\mathbf{Z}}_i\\ \underline{\mathbf{U}}_{i,2i-1}\end{array}\right] + \underline{\mathbf{\Psi}}_i \in \Re^{(n+mp)\times N},$$

  where $\underline{\mathbf{\Gamma}}_i^+$ is the Moore-Penrose pseudo inverse of $\underline{\mathbf{\Gamma}}_i$ with rank of n; $\underline{\mathbf{\Psi}}_i$ is the error matrix; and $\underline{\mathbf{Y}}_{i,i} = \left[\begin{array}{cccc}\underline{\mathbf{y}}(i) & \underline{\mathbf{y}}(i+1) & \cdots & \underline{\mathbf{y}}(i+N-1)\end{array}\right] \in \Re^{mp\times N}$.

- The system matrices are determined as $\underline{\mathbf{A}} \leftarrow \mathbf{K}_1(1:n,:)$, $\underline{\mathbf{C}} \leftarrow \mathbf{K}_1(n+1:mp+n,:)$, where the MATLAB notation to represent a submatrix has been employed. In addition,

$$\mathbf{K}_2 = \left[\begin{array}{cc}\underline{\mathbf{B}} - \underline{\mathbf{A}}\ \underline{\mathbf{\Gamma}}_i^+\left[\begin{array}{c}\underline{\mathbf{D}}\\ \underline{\mathbf{\Gamma}}_{i-1}\underline{\mathbf{B}}\end{array}\right] & \underline{\mathbf{\Gamma}}_{i-1}^+\underline{\mathbf{H}}_{i-1} - \underline{\mathbf{A}}\ \underline{\mathbf{\Gamma}}_i^+\left[\begin{array}{c}\mathbf{0}\\ \underline{\mathbf{H}}_{i-1}\end{array}\right]\\ \underline{\mathbf{D}} - \underline{\mathbf{C}}\ \underline{\mathbf{\Gamma}}_i^+\left[\begin{array}{c}\underline{\mathbf{D}}\\ \underline{\mathbf{\Gamma}}_{i-1}\underline{\mathbf{B}}\end{array}\right] & -\underline{\mathbf{C}}\ \underline{\mathbf{\Gamma}}_i^+\left[\begin{array}{c}\mathbf{0}\\ \underline{\mathbf{H}}_{i-1}\end{array}\right]\end{array}\right] \in \Re^{(n+mp)\times ilg}.$$

  Observe that $\underline{\mathbf{B}}$ and $\underline{\mathbf{D}}$ linearly appear in $\mathbf{K}_2(:,1:lg)$. Therefore, by constructing a set of linear equations, we can solve $\underline{\mathbf{B}}$ and $\underline{\mathbf{D}}$ as in Verhaegen (1994).

- From $\underline{\mathbf{\Psi}}_i$, calculating its covariance matrix results in

$$\left[\begin{array}{cc}\mathbf{R}_\omega & \mathbf{R}'_{\omega,\varepsilon}\\ \underline{\mathbf{R}}_{\omega,\varepsilon} & \underline{\mathbf{R}}_\varepsilon\end{array}\right] \Leftarrow \frac{1}{N-1}\underline{\mathbf{\Psi}}_i\underline{\mathbf{\Psi}}_i'.$$

4 Kalman Filter for the NUSM System

Suppose that $\{\underline{\mathbf{A}}, \underline{\mathbf{B}}, \underline{\mathbf{C}}, \underline{\mathbf{D}}\}$, $\underline{\mathbf{R}}_\omega$, $\underline{\mathbf{R}}_\varepsilon$, and $\underline{\mathbf{R}}_{\varepsilon,\omega}$ have been identified. Denote $\hat{\mathbf{x}}(k|j)$ as the estimate of $\mathbf{x}(k)$ based on data $\{\underline{\mathbf{u}}(1), \underline{\mathbf{y}}(1), \cdots, \underline{\mathbf{u}}(j), \underline{\mathbf{y}}(j)\}$, where $j = k-1$ or $j = k$. The Kalman filter for the NUSM system represented by Eqn. 5 should enable the estimation of $\mathbf{x}(k)$ such that $\mathbf{x}(k) - \hat{\mathbf{x}}(k|j)$ has minimized covariance. Specifically, the Kalman filter functions as a one step prediction algorithm if $j = k-1$, or a filtering algorithm if $j = k$.

4.1 The one-step prediction algorithm

Let the one-step prediction algorithm have the following form (Aström, 1970; Chen et al., 1995) :

$$\hat{\mathbf{x}}(k+1|k) = \underline{\mathbf{A}}\,\hat{\mathbf{x}}(k|k-1) + \underline{\mathbf{B}}\,\underline{\mathbf{u}}(k) + \underline{\mathbf{L}}(k)\left[\underline{\mathbf{y}}(k) - \underline{\mathbf{C}}\,\hat{\mathbf{x}}(k|k-1) - \underline{\mathbf{D}}\,\underline{\mathbf{u}}(k)\right] \quad (7)$$

where $\hat{\mathbf{x}}(k+1|k)$ is similarly defined as $\hat{\mathbf{x}}(k|k-1)$, and $\underline{\mathbf{L}}(k)$ is the Kalman gain to be determined later. Define $\bar{\mathbf{x}}(i|i-1) \equiv \mathbf{x}(i) - \hat{\mathbf{x}}(i|i-1)$ as the estimation error, for $i = k$ or $i = k+1$. Accordingly, we are led to

$$\bar{\mathbf{x}}(k+1|k) = [\underline{\mathbf{A}} - \underline{\mathbf{L}}(k)\underline{\mathbf{C}}]\,\bar{\mathbf{x}}(k|k-1) + \underline{\boldsymbol{\omega}}(k) - \underline{\mathbf{L}}(k)\underline{\boldsymbol{\varepsilon}}(k) \quad (8)$$

Define $\underline{\mathbf{M}}(k) \equiv E\left(\{\bar{\mathbf{x}}(k|k-1) - E\left[\bar{\mathbf{x}}(k|k-1)\right]\}\{\bar{\mathbf{x}}(k|k-1) - E\left[\bar{\mathbf{x}}(k|k-1)\right]\}'\right)$ as the covariance matrix of $\bar{\mathbf{x}}(k|k-1)$, where $E\{\ \}$ is the expectation of the argument. If one chooses $\hat{\mathbf{x}}(0|-1) = E\mathbf{x}(0)$, then $E\left[\bar{\mathbf{x}}(0|-1)\right] = E[\mathbf{x}(0) - \hat{\mathbf{x}}(0|-1)] = \mathbf{0}$. It follows from Eqn. 8 that $E[\bar{\mathbf{x}}(k+1|k)] = [\underline{\mathbf{A}} - \underline{\mathbf{L}}(k)\underline{\mathbf{C}}]\,E[\bar{\mathbf{x}}(k|k-1)$, where $E\{\underline{\boldsymbol{\omega}}(k) - \underline{\mathbf{L}}(k)\underline{\boldsymbol{\varepsilon}}(k)\} = \mathbf{0}$. By repeating recursions, one can show $E\left[\bar{\mathbf{x}}(k|k-1)\right] = \prod_{i=0}^{k-1}[\underline{\mathbf{A}} - \underline{\mathbf{L}}(i)\underline{\mathbf{C}}]\,E\left[\bar{\mathbf{x}}(0|-1)\right]$. Consequently, $\underline{\mathbf{M}}(k) = E\left[\bar{\mathbf{x}}(k|k-1)\bar{\mathbf{x}}'(k|k-1)\right]$. It turns out also from Eqn. 8 that

$$\begin{aligned}\underline{\mathbf{M}}(k+1) &= E[\bar{\mathbf{x}}(k+1|k)\bar{\mathbf{x}}'(k+1|k)] \quad (9)\\ &= [\underline{\mathbf{A}} - \underline{\mathbf{L}}(k)\underline{\mathbf{C}}]\,\underline{\mathbf{M}}(k)\,[\underline{\mathbf{A}} - \underline{\mathbf{L}}(k)\underline{\mathbf{C}}]' + E\{[\underline{\boldsymbol{\omega}}(k) - \underline{\mathbf{L}}(k)\underline{\boldsymbol{\varepsilon}}(k)][\underline{\boldsymbol{\omega}}(k) - \underline{\mathbf{L}}(k)\underline{\boldsymbol{\varepsilon}}(k)]'\}\end{aligned}$$

where the independence between $\bar{\mathbf{x}}(k|k-1)$ and $\underline{\boldsymbol{\varepsilon}}(k)/\underline{\boldsymbol{\omega}}(k)$ has been taken into account.

In the development of the Kalman filter, the criterion is to minimize the trace of $\underline{\mathbf{M}}(k+1)$, $\mathrm{Tr}\{\underline{\mathbf{M}}(k+1)\}$. We can prove that $\underline{\mathbf{M}}(k+1)$ is non-negative definite. Consequently, the minimization of $\mathrm{Tr}\{\underline{\mathbf{M}}(k+1)\}$ is equivalent to that of the following non-negative scalar:

$$\begin{aligned}\boldsymbol{\alpha}'\underline{\mathbf{M}}(k+1)\boldsymbol{\alpha} &= \boldsymbol{\alpha}' E\{[\underline{\boldsymbol{\omega}}(k) - \underline{\mathbf{L}}(k)\underline{\boldsymbol{\varepsilon}}(k)][\underline{\boldsymbol{\omega}}(k) - \underline{\mathbf{L}}(k)\underline{\boldsymbol{\varepsilon}}(k)]'\}\boldsymbol{\alpha}\\ &+ \boldsymbol{\alpha}'\{[\underline{\mathbf{A}} - \underline{\mathbf{L}}(k)\underline{\mathbf{C}}]\,\underline{\mathbf{M}}(k)\,[\underline{\mathbf{A}} - \underline{\mathbf{L}}(k)\underline{\mathbf{C}}]'\}\boldsymbol{\alpha},\end{aligned}$$

where $\boldsymbol{\alpha}$ is an arbitrary non-zero vector. Using derivations similar to those in Aström (1970), we obtain the optimal solution of $\underline{\mathbf{L}}(k)$ to minimize $\boldsymbol{\alpha}'\underline{\mathbf{M}}(k+1)\boldsymbol{\alpha}$ as follows:

$$\underline{\mathbf{L}}(k) = \left[\underline{\mathbf{A}}\,\underline{\mathbf{M}}(k)\underline{\mathbf{C}}' + \underline{\mathbf{R}}_{\omega,\varepsilon}\right]\underline{\mathbf{H}}^{-1}(k) \quad (10)$$

where $\underline{\mathbf{H}}(k) = \underline{\mathbf{C}}\ \underline{\mathbf{M}}(k)\underline{\mathbf{C}}' + \underline{\mathbf{R}}_{\varepsilon}$ is positive definite, because $\underline{\mathbf{R}}_{\varepsilon}$ is positive definite and $\underline{\mathbf{C}}\ \underline{\mathbf{M}}(k)\underline{\mathbf{C}}'$ is non-negative definite. Accordingly, Eqn. 9 can be rewritten as

$$\underline{\mathbf{M}}(k+1) = \underline{\mathbf{A}}\ \underline{\mathbf{M}}(k)\underline{\mathbf{A}}' + \underline{\mathbf{R}}_{\omega} - \left[\underline{\mathbf{A}}\ \underline{\mathbf{M}}(k)\underline{\mathbf{C}}' + \underline{\mathbf{R}}_{\omega,\varepsilon}\right] \underline{\mathbf{H}}^{-1}(k) \left[\underline{\mathbf{A}}\ \underline{\mathbf{M}}(k)\underline{\mathbf{C}}' + \underline{\mathbf{R}}_{\omega,\varepsilon}\right]' \quad (11)$$

At last, we define

$$\underline{\bar{\mathbf{y}}}(k|k-1) \equiv \underline{\mathbf{y}}(k) - \underline{\hat{\mathbf{y}}}(k|k-1) = \underline{\mathbf{C}}\left[\underline{\bar{\mathbf{x}}}(k|k-1)\right] + \underline{\boldsymbol{\varepsilon}}(k) \quad (12)$$

as the innovation vector, where $\underline{\hat{\mathbf{y}}}(k|k-1) = \underline{\mathbf{C}}\underline{\hat{\mathbf{x}}}(k|k-1) + \underline{\mathbf{D}}\ \underline{\mathbf{u}}(k)$ is the prediction of $\underline{\mathbf{y}}(k)$. Similar to Haykin (1996), we can prove that the innovation is a white noise vector with covariance $Cov[\underline{\bar{\mathbf{y}}}(k|k-1)] = \underline{\mathbf{H}}(k)$.

Eqns. 7, 10, 11, and 12 construct the one-step prediction algorithm of the Kalman filer given a system described by Eqn. 5. And the initial conditions are $\hat{\mathbf{x}}(0|-1) = E[\mathbf{x}(0)]$ and $\underline{\mathbf{M}}(0) = E[\bar{\mathbf{x}}(0|-1)\bar{\mathbf{x}}'(0|-1)]$. The estimated states $\hat{\mathbf{x}}(k|k-1)$ are unbiased, i.e. $E\left[\hat{\mathbf{x}}(k|k-1)\right] = E[\mathbf{x}(k)]$, because $E\left[\bar{\mathbf{x}}(k|k-1)\right] = \mathbf{0}$.

4.2 Stability and convergence analysis

We analyze the stability and convergence of the one step prediction algorithm by applying the well known results in de Souza et al. (1986). The algebraic Ricatti difference equation (ARDE) for the Kalman filter is given by Eqn. 11. The NUSM system of Eqn. 5 has preserved the causality, observability and controllability of the original CT system of Eqn. 1. Accordingly, (i) the pair $(\underline{\mathbf{A}}, \underline{\mathbf{C}})$ is detectable; and (ii) there exists no unreachable mode of $\left(\underline{\mathbf{A}}, \underline{\mathbf{R}}_{\omega}^{1/2}\right)$ on the unit circle. Under these conditions and with $\underline{\mathbf{M}}(0) > \mathbf{0}$, the ARDE has unique stabilizing solution $\underline{\mathbf{M}}(k)$ (poles of steady state values of $\underline{\mathbf{A}} - \underline{\mathbf{L}}(k)\underline{\mathbf{C}}$ are inside or on the stability boundary), and the sequence $\underline{\mathbf{M}}(k)$ converges exponentially to $\underline{\mathbf{M}}(\infty)$ (de Souza et al., 1986).

4.3 The filtering algorithm

A complete Kalamn filter should also include the filtering algorithm, which is usually employed to de-noise measured variables. In filtering, the goal is to compute the estimate, $\hat{\mathbf{x}}(k|k)$, from $\{\underline{\mathbf{u}}(1), \underline{\mathbf{y}}(1), \cdots, \underline{\mathbf{u}}(k), \underline{\mathbf{y}}(k)\}$, such that $\hat{\mathbf{x}}(k|k) - \mathbf{x}(k)$ has minimized covariance.

Geometrically, $\hat{\mathbf{x}}(k|k)$ is the minimum mean-square projection of $\mathbf{x}(k)$ onto the space spanned by observations: $\underline{\mathbf{Z}}_{1:k} \equiv [\underline{\mathbf{z}}(1) \cdots \underline{\mathbf{z}}(k)] \in \Re^{mp \times k}$, where $\underline{\mathbf{z}}(i) = \underline{\mathbf{y}}(i) - \underline{\mathbf{D}}\ \underline{\mathbf{u}}(i) \in \Re^{mp}$, for $i \in [1, k]$. Denote $\hat{\mathbf{x}}(k|k) \equiv \hat{\mathbf{x}}(k|_{\underline{\mathbf{Z}}_{1:k}})$. We can infer that a one-to-one correspondence exists between $\underline{\mathbf{z}}(k)$ and $\bar{\underline{\mathbf{y}}}(k|k-1)$, $\forall\ k$, by extending the analysis in Haykin (1996). As a consequence, $\underline{\mathbf{Z}}_{1:k} = [\underline{\mathbf{Z}}_{1:k-1}\ \underline{\mathbf{z}}(k)] = \underline{\mathbf{Z}}_{1:k-1} \oplus \bar{\underline{\mathbf{y}}}(k|k-1)$, where $\underline{\mathbf{Z}}_{1:k-1} = [\underline{\mathbf{z}}(1) \cdots \underline{\mathbf{z}}(k-1)] \in \Re^{mp \times (k-1)}$ is also a subspace, and $\oplus$ stands for the sum of two subspaces. Furthermore, applying the principle of orthogonality (Haykin, 1996) can show the orthogonality between $\bar{\underline{\mathbf{y}}}(k|k-1)$ and $\underline{\mathbf{Z}}_{1:i}$, $\forall\ 1 \leq i \leq k-1$. Thus $\underline{\mathbf{Z}}_{1:k}$ is the direct sum of $\underline{\mathbf{Z}}_{1:k-1}$ and $\bar{\underline{\mathbf{y}}}(k|k-1)$. Accordingly,

$$\hat{\mathbf{x}}(k|k) = \hat{\mathbf{x}}(k|_{\underline{\mathbf{Z}}_{1:k-1}}) + \hat{\mathbf{x}}(k|_{\bar{\underline{\mathbf{y}}}(k|k-1)}) = \hat{\mathbf{x}}(k|k-1) + \underline{\mathbf{N}}(k)\bar{\underline{\mathbf{y}}}(k|k-1) \tag{13}$$

where $\hat{\mathbf{x}}(k|k-1) = \hat{\mathbf{x}}(k|_{\underline{\mathbf{Z}}_{1:k-1}})$, $\hat{\mathbf{x}}(k|_{\bar{\underline{\mathbf{y}}}(k|k-1)}) = \underline{\mathbf{N}}(k)\ \bar{\underline{\mathbf{y}}}(k|k-1)$ is the mean-square projection of $\mathbf{x}(k)$ onto $\bar{\underline{\mathbf{y}}}(k|k-1)$, and $\underline{\mathbf{N}}(k)$ is a gain matrix to be determined later.

The substitution of Eqn. 12 into Eqn. 13 leads to $\hat{\mathbf{x}}(k|k) = \hat{\mathbf{x}}(k|k-1) + \underline{\mathbf{N}}(k)[\underline{\mathbf{C}}\ \bar{\underline{\mathbf{x}}}(k|k-1) + \underline{\boldsymbol{\varepsilon}}(k)]$, resulting in,

$$\bar{\mathbf{x}}(k|k) = \mathbf{x}(k) - \hat{\mathbf{x}}(k|k) = [\mathbf{I}_n - \underline{\mathbf{N}}(k)\underline{\mathbf{C}}]\,\bar{\mathbf{x}}(k|k-1) - \underline{\mathbf{N}}(k)\underline{\boldsymbol{\varepsilon}}(k) \tag{14}$$

We can show $E[\bar{\mathbf{x}}(k|k)] = \mathbf{0}$. Therefore, the covariance of $\bar{\mathbf{x}}(k|k)$ is

$$\begin{aligned} Cov\,[\bar{\mathbf{x}}(k|k)] &= E\,[\bar{\mathbf{x}}(k|k)\bar{\mathbf{x}}'(k|k)] \\ &= [\mathbf{I} - \underline{\mathbf{N}}(k)\underline{\mathbf{C}}]\,\underline{\mathbf{M}}(k)\,[\mathbf{I} - \underline{\mathbf{N}}(k)\underline{\mathbf{C}}]' + \underline{\mathbf{N}}(k)\ \underline{\mathbf{R}}_{\varepsilon}\ \underline{\mathbf{N}}'(k) \end{aligned} \tag{15}$$

where Eqn. 14, the definition of $\underline{\mathbf{M}}(k)$, and $E\,[\bar{\mathbf{x}}(k|k-1)\underline{\boldsymbol{\varepsilon}}'(k)] = \mathbf{0}$ have been utilized.

The right hand side of Eqn. 15 can be converted as $\underline{\mathbf{M}}(k) - \underline{\mathbf{M}}(k)\underline{\mathbf{C}}'\underline{\mathbf{H}}^{-1}(k)\underline{\mathbf{C}}\ \underline{\mathbf{M}}(k) + [\underline{\mathbf{N}}(k) - \underline{\mathbf{M}}(k)\underline{\mathbf{C}}'\underline{\mathbf{H}}^{-1}(k)]\underline{\mathbf{H}}(k)[\underline{\mathbf{N}}(k) - \underline{\mathbf{M}}(k)\underline{\mathbf{C}}'\underline{\mathbf{H}}^{-1}(k)]'$, where the first term is independent of $\underline{\mathbf{N}}(k)$. Therefore, the trace of $Cov[\bar{\mathbf{x}}(k|k)]$ reaches its minimum when the non-negative definite term, $[\underline{\mathbf{N}}(k) - \underline{\mathbf{M}}(k)\underline{\mathbf{C}}'\underline{\mathbf{H}}^{-1}(k)]\underline{\mathbf{H}}(k)[\underline{\mathbf{N}}(k) - \underline{\mathbf{M}}(k)\underline{\mathbf{C}}'\underline{\mathbf{H}}^{-1}(k)]'$, is zero. This gives the optimal solution to $\underline{\mathbf{N}}(k)$ as follows,

$$\underline{\mathbf{N}}(k) = \underline{\mathbf{M}}(k)\underline{\mathbf{C}}'\ \underline{\mathbf{H}}^{-1}(k) \tag{16}$$

which in turn results in $Cov\,[\bar{\mathbf{x}}(k|k)] = \underline{\mathbf{M}}(k) - \underline{\mathbf{M}}(k)\underline{\mathbf{C}}'\underline{\mathbf{H}}^{-1}(k)\underline{\mathbf{C}}\,\underline{\mathbf{M}}(k)$. Finally, with $\hat{\mathbf{x}}(k|k)$,

$$\underline{\hat{\mathbf{y}}}(k|k) = \underline{\mathbf{C}}\hat{\mathbf{x}}(k|k) + \underline{\mathbf{D}}\;\underline{\mathbf{u}}(k), \quad \underline{\bar{\mathbf{y}}}(k|k) = \mathbf{y}(k) - \underline{\hat{\mathbf{y}}}(k|k) = \underline{\mathbf{C}}\bar{\mathbf{x}}(k|k) + \underline{\boldsymbol{\varepsilon}}(k) \tag{17}$$

Eqns. 13, 16, and 17 plus the earlier developed one step prediction algorithm constitute the Kalman filtering algorithm.

5 Kalman filter-based FDI in the NUSM system

In this section, a novel Kalman filter-based FDI methodology is investigated, which gives a unified treatment of faults in sensors, process components and actuators. This is in contrast to most of the existing Kalman filter-based FDI schemes, which only work for process faults or actuator faults but not for sensor faults (White and Speyer, 1984) due to their fundamental limitations.

5.1 Mathematical description of the NUSM system with faults

While a MIMO system can be represented by Eqn. 1 in the fault-free case, in the presence of process faults the system should be represented by (Li et al., 2003)

$$\dot{\mathbf{x}}(t) = \mathbf{A}\mathbf{x}(t) + \mathbf{B}\tilde{\mathbf{u}}(t) + \mathbf{f}_p(t) + \boldsymbol{\phi}(t), \quad \tilde{\mathbf{y}}(t) = \mathbf{C}\mathbf{x}(t) + \mathbf{D}\tilde{\mathbf{u}}(t) \tag{18}$$

In Eqn. 18, $\mathbf{f}_p(t) \in \Re^n$ is the fault magnitude vector with zero or non-zero elements. Consider the following quadruple tank system shown in Figure 2 as an example, where leaks in each tank, denoted by $\{\delta_1, \delta_2, \delta_3, \delta_4\}$, are typical process faults. In this system, if only one tank, e.g. Tank 1, leaks, $\mathbf{f}_p(t) = [\delta_1\ 0\ 0\ 0]'$. If two tanks, e.g. Tanks 2 and 4, leak simultaneously, then $\mathbf{f}_p(t) = [0\ \delta_2\ 0\ \delta_4]'$. In addition, any other leak scenarios can be similarly represented in terms of $\mathbf{f}_p(t)$.

We apply the NUSM sampling approach to discretize Eqn. 18, where $\mathbf{f}_p(t)$ is "sampled" at the same rate as the process disturbance $\boldsymbol{\phi}(t)$. Similarly, we can show that the resulting lifted model is

$$\mathbf{x}(k+1) = \underline{\mathbf{A}}\;\mathbf{x}(k) + \underline{\mathbf{B}}\;\tilde{\underline{\mathbf{u}}}(k) + \underline{\mathbf{W}}\;\underline{\mathbf{f}}_p(k) + \underline{\mathbf{W}}\;\underline{\boldsymbol{\phi}}(k), \quad \tilde{\underline{\mathbf{y}}}(k) = \underline{\mathbf{C}}\;\mathbf{x}(k) + \underline{\mathbf{D}}\;\tilde{\underline{\mathbf{u}}}(k) \tag{19}$$

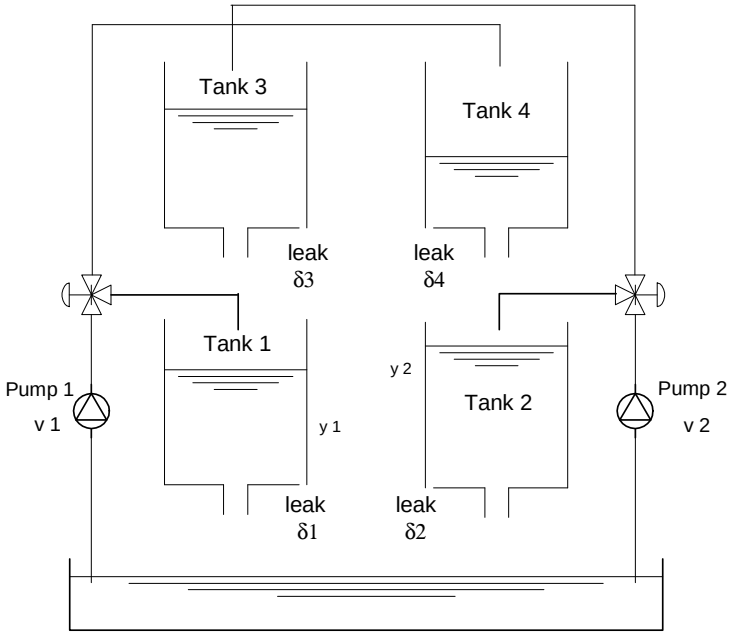

Figure 2: Schematic of the quadruple tank system

where $\underline{\mathbf{f}}_p(k) \in \Re^{ng}$ is the lifted vector of $\mathbf{f}_p(t)$ and analogous to $\underline{\phi}(k)$ in structure.

We also consider the presence of faults in actuators and sensors in Eqn. 19 as depicted by Figure 3. Therein, the measured outputs of the system with sensor faults are $\mathbf{y}(kT + t_i) =$

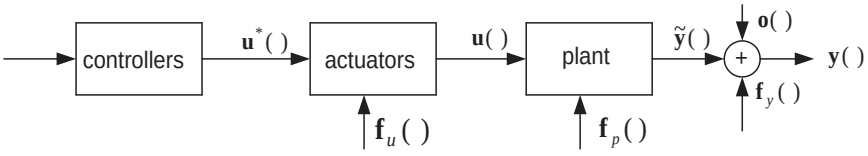

Figure 3: *Schematic diagram of a system with faults in actuator, process components and sensors*

$\mathbf{y}^*(kT+t_i)+\mathbf{f}_y(kT+t_i)$, where $\mathbf{y}^*(kT+t_i) = \tilde{\mathbf{y}}(kT+t_i)+\mathbf{o}(kT+t_i)$ is the fault-free value, and $\mathbf{f}_y(\ )$ is the fault magnitude vector similar to $\mathbf{f}_p(\ )$. For instance, if the first and third sensors are faulty, the first and third elements in $\mathbf{f}_y(kT + t_i)$ are non-zero, while other elements are zero. The inputs to the plant in Figure 3 are $\mathbf{u}(kT + t_i^j) = \mathbf{u}^*(kT + t_i^j) + \mathbf{f}_u(kT + t_i^j)$, where, for $j = [1, n_i]$, $\mathbf{u}^*(kT + t_i^j)$ are the fault-free values; $\mathbf{f}_u(kT + t_i^j)$ is the fault vector in the actuators and analogous to $\mathbf{f}_p(\ )$ ($\mathbf{f}_y(\ )$) in structure. While $\mathbf{u}^*(kT + t_i^j)$ are available (they are outputs of controllers), $\mathbf{u}(kT + t_i^j)$ are not.

We define $\underline{\mathbf{u}}(k) = \underline{\mathbf{u}}^*(k) + \underline{\mathbf{f}}_u(k) \in \Re^{lg}$, $\underline{\mathbf{y}}(k) = \underline{\mathbf{y}}^*(k) + \underline{\mathbf{f}}_y(k) = \underline{\tilde{\mathbf{y}}}(k) + \underline{\mathbf{o}}(k) + \underline{\mathbf{f}}_y(k) \in \Re^{mp}$, where $\underline{\mathbf{f}}_y(k)$ is similarly defined as $\underline{\mathbf{y}}(k)$ ($\underline{\mathbf{y}}^*(k)$), and so is $\underline{\mathbf{f}}_u(k)$ to $\underline{\mathbf{u}}(k)$ ($\underline{\mathbf{u}}^*(k)$). Accordingly, we rewrite Eqn. 19 as

$$\begin{aligned} \mathbf{x}(k+1) &= \underline{\mathbf{A}}\ \mathbf{x}(k) + \underline{\mathbf{B}}\ \underline{\mathbf{u}}^*(k) + \underline{\mathbf{B}}\ \underline{\mathbf{f}}_u(k) + \underline{\mathbf{W}}\ \underline{\mathbf{f}}_p(k) + \underline{\boldsymbol{\omega}}(k) \\ \underline{\mathbf{y}}(k) &= \underline{\mathbf{C}}\ \mathbf{x}(k) + \underline{\mathbf{D}}\ \underline{\mathbf{u}}^*(k) + \underline{\mathbf{D}}\ \underline{\mathbf{f}}_u(k) + \underline{\mathbf{f}}_y(k) + \underline{\boldsymbol{\varepsilon}}(k) \end{aligned} \tag{20}$$

which describes the dynamics of the NUSM system in the presence of noise, disturbances, and faults. With Eqn. 20, we state the FDI problem as follows:

Given data: $\{\mathbf{u}^*(kT + t_i^j)\}$ and $\{\mathbf{y}(kT + t_i)\}$, for $i = [1, p]$, $j = [1, n_i]$, and $k = [1, 2, \cdots]$, FDI is to indicate when and which element(s) in $\mathbf{f}_p(\ )$, $\mathbf{f}_u(\ )$, and/or $\mathbf{f}_y(\ )$ begin to be non-zero.

5.2 Fault detection in the NUSM system

We substitute Eqn. 20 into the one step prediction algorithm, where $\underline{\mathbf{L}}(k)$ is replaced by its steady value, $\underline{\mathbf{L}}$. Consequently,

$$\begin{aligned} \hat{\mathbf{x}}(k+1|k) &= \underline{\mathbf{A}}\ \hat{\mathbf{x}}(k|k-1) + \underline{\mathbf{B}}\ \underline{\mathbf{u}}^*(k) + \underline{\mathbf{L}}\ \bar{\mathbf{y}}(k|k-1) \\ \underline{\hat{\mathbf{y}}}(k|k-1) &= \underline{\mathbf{C}}\ \hat{\mathbf{x}}(k|k-1) + \underline{\mathbf{D}}\ \underline{\mathbf{u}}^*(k) \end{aligned} \tag{21}$$

where $\underline{\bar{\mathbf{y}}}(k|k-1) = \underline{\mathbf{C}}\bar{\mathbf{x}}(k|k-1) + \underline{\mathbf{D}}\ \underline{\mathbf{f}}_u(k) + \underline{\mathbf{f}}_y(k) + \underline{\boldsymbol{\varepsilon}}(k)$. Subtracting Eqn. 20 by Eqn. 21 produces $\bar{\mathbf{x}}(k+1|k) = \underline{\bar{\mathbf{A}}}\ \underline{\mathbf{C}}\ \bar{\mathbf{x}}(k|k-1) + \underline{\bar{\mathbf{B}}}\ \underline{\mathbf{f}}_u(k) - \underline{\mathbf{L}}\ \underline{\mathbf{f}}_y(k) + \underline{\mathbf{W}}\ \underline{\mathbf{f}}_p(k) + \underline{\boldsymbol{\omega}}(k) - \underline{\mathbf{L}}\ \underline{\boldsymbol{\varepsilon}}(k)$, where $\underline{\bar{\mathbf{A}}} \equiv \underline{\mathbf{A}} - \underline{\mathbf{L}}\ \underline{\mathbf{C}}$ and $\underline{\bar{\mathbf{B}}} \equiv \underline{\mathbf{B}} - \underline{\mathbf{L}}\ \underline{\mathbf{D}}$.

From the preceding equation it can be shown that

$$\bar{\mathbf{x}}(k|k-1) = \bar{\mathbf{x}}^*(k|k-1) + \bar{\mathbf{x}}^f(k|k-1) \tag{22}$$

where, $\bar{\mathbf{x}}^*(k|k-1) = \underline{\bar{\mathbf{A}}}^k \bar{\mathbf{x}}(0|-1) + \sum_{i=0}^{k-1} \underline{\bar{\mathbf{A}}}^{k-1-i} [\underline{\boldsymbol{\omega}}(i) - \underline{\mathbf{L}}\ \underline{\boldsymbol{\varepsilon}}(i)]$, and

$$\bar{\mathbf{x}}^f(k|k-1) = \sum_{i=0}^{k-1} \underline{\bar{\mathbf{A}}}^{k-1-i} [\underline{\bar{\mathbf{B}}}\ \underline{\mathbf{f}}_u(i) - \underline{\mathbf{L}}\ \underline{\mathbf{f}}_y(i) + \underline{\mathbf{W}}\ \underline{\mathbf{f}}_p(i)].$$

Finally, the substitution of Eqn. 22 into Eqn. 21 produces

$$\underline{\bar{\mathbf{y}}}(k|k-1) = \underline{\bar{\mathbf{y}}}^*(k|k-1) + \underline{\bar{\mathbf{y}}}^f(k|k-1) \tag{23}$$

where $\underline{\bar{\mathbf{y}}}^*(k|k-1) = \underline{\mathbf{C}}\ \underline{\bar{\mathbf{A}}}^k \bar{\mathbf{x}}(0|-1) + \underline{\mathbf{C}} \sum_{i=0}^{k-1} \underline{\bar{\mathbf{A}}}^{k-1-i} [\underline{\boldsymbol{\omega}}(i) - \underline{\mathbf{L}}\ \underline{\boldsymbol{\varepsilon}}(i)\ ] + \underline{\boldsymbol{\varepsilon}}(k) \sim \aleph[\mathbf{0}, \underline{\mathbf{H}}(k)]$ (Haykin, 1996); and $\underline{\bar{\mathbf{y}}}^f(k|k-1) = \underline{\mathbf{C}} \sum_{i=0}^{k-1} \underline{\bar{\mathbf{A}}}^{k-1-i} [\underline{\bar{\mathbf{B}}}\ \underline{\mathbf{f}}_u(i) - \underline{\mathbf{L}}\ \underline{\mathbf{f}}_y(i) + \underline{\mathbf{W}}\ \underline{\mathbf{f}}_p(i)] + \underline{\mathbf{D}}\ \underline{\mathbf{f}}_u(k) + \underline{\mathbf{f}}_y(k)$.

It has been shown in Section 4.2 that $\underline{\bar{\mathbf{A}}}$ has stable eigenvalues. With eigen decomposition: $\underline{\bar{\mathbf{A}}} = \underline{\mathbf{U}}_A \underline{\boldsymbol{\Lambda}}_A \underline{\mathbf{U}}_A^{-1}$, where $\underline{\boldsymbol{\Lambda}}_A$ is a diagonal matrix containing all the non-zero eigenvalues and $\underline{\mathbf{U}}_A$ are the associated eigenvectors, we can rewrite Eqn. 23 as

$$\begin{aligned} \underline{\bar{\mathbf{y}}}^f(k|k-1) &= \underline{\mathbf{C}}\ \underline{\mathbf{U}}_A \sum_{i=0}^{k-2} \underline{\boldsymbol{\Lambda}}_A^{k-1-i} \underline{\mathbf{U}}_A^{-1} [\underline{\bar{\mathbf{B}}}\ \underline{\mathbf{f}}_u(i) - \underline{\mathbf{L}}\ \underline{\mathbf{f}}_y(i) + \underline{\mathbf{W}}\ \underline{\mathbf{f}}_p(i)] \\ &+ \underline{\mathbf{C}}[\underline{\bar{\mathbf{B}}}\ \underline{\mathbf{f}}_u(k-1) - \underline{\mathbf{L}}\ \underline{\mathbf{f}}_y(k-1) + \underline{\mathbf{W}}\ \underline{\mathbf{f}}_p(k-1)] + \underline{\mathbf{D}}\ \underline{\mathbf{f}}_u(k) + \underline{\mathbf{f}}_y(k). \end{aligned}$$

Select a matrix, $\underline{\mathbf{W}}_\circ$, from the left null space of $\underline{\mathbf{C}}\ \underline{\mathbf{U}}_A$, i.e. $\underline{\mathbf{W}}_\circ \underline{\mathbf{C}}\ \underline{\mathbf{U}}_A \equiv \mathbf{0}$. Multiplying $\underline{\bar{\mathbf{y}}}(k|k-1)$ by $\underline{\mathbf{W}}_\circ$, we define

$$\underline{\mathbf{e}}(k) \equiv \underline{\mathbf{W}}_\circ \underline{\bar{\mathbf{y}}}(k|k-1) = \underline{\mathbf{e}}^*(k) + \underline{\mathbf{e}}^f(k) \tag{24}$$

as the primary residual vector (PRV) for fault detection, where $\underline{\mathbf{e}}^*(k) = \underline{\mathbf{W}}_\circ \underline{\bar{\mathbf{y}}}^*(k|k-1) = \underline{\mathbf{W}}_\circ\ \underline{\mathbf{C}}[\mathbf{I}_{mp}| - \underline{\mathbf{L}}][\underline{\boldsymbol{\omega}}'(k-1)\ \underline{\boldsymbol{\varepsilon}}'(k-1)]' + \underline{\mathbf{W}}_\circ\ \underline{\boldsymbol{\varepsilon}}(k)$ is the fault-free component, while

$$\begin{aligned} \underline{\mathbf{e}}^f(k) &= \underline{\mathbf{W}}_\circ \underline{\bar{\mathbf{y}}}^f(k|k-1) \\ &= \underline{\mathbf{W}}_\circ [\underline{\mathbf{D}}\ |\underline{\mathbf{C}}\ \underline{\bar{\mathbf{B}}}\ |\underline{\mathbf{C}}\ \underline{\mathbf{W}}\ |\ \mathbf{I}_{mp}| - \underline{\mathbf{C}}\ \underline{\mathbf{L}}] \left[\ \underline{\mathbf{f}}_u'(k)\ \underline{\mathbf{f}}_u'(k-1)\ \underline{\mathbf{f}}_p'(k-1)\ \underline{\mathbf{f}}_y'(k)\ \underline{\mathbf{f}}_y'(k-1)\ \right]' \end{aligned}$$

is the fault-contribution component. Note that $\underline{\mathbf{e}}^*(k)$ only has terms with constant coefficients. Therefore, it is a stationary white noise vector. We can show that $\underline{\mathbf{e}}^*(k) \sim \aleph[\mathbf{0}, \underline{\mathbf{R}}_e]$, where $\underline{\mathbf{R}}_e = \underline{\mathbf{W}}_\circ \underline{\mathbf{H}}(\infty) \underline{\mathbf{W}}_\circ' \in \Re^{n_0 \times n_0}$ with $\underline{\mathbf{H}}(\infty)$ being the steady value of $\underline{\mathbf{H}}(k)$.

No matter what the order, n, of the system is, $\underline{\mathbf{e}}^f(k)$ is always a first order moving average (MA) process of $\underline{\mathbf{f}}_u(k)$, $\underline{\mathbf{f}}_y(k)$, and $\underline{\mathbf{f}}_p(k)$. This ensures simplicity of the PRV. In $\mathbf{e}^f(k)$, denote the gain between $\underline{\mathbf{W}}_\circ$ and $\left[\ \underline{\mathbf{f}}_u'(k)\ \underline{\mathbf{f}}_u'(k-1)\ \underline{\mathbf{f}}_p'(k-1)\ \underline{\mathbf{f}}_y'(k-1)\ \right]'$ by $\underline{\boldsymbol{\Theta}}_1 \equiv [\underline{\mathbf{D}}\ |\ \underline{\mathbf{C}}\ \underline{\bar{\mathbf{B}}}|\underline{\mathbf{C}}\ \underline{\mathbf{W}}| - \underline{\mathbf{C}}\ \underline{\mathbf{L}}]$. Besides $\underline{\mathbf{W}}_\circ \underline{\mathbf{C}}\ \underline{\mathbf{U}}_A = \mathbf{0}$, each row of $\underline{\mathbf{W}}_\circ$ should be designed such that the ratio

$$\lambda_i = \frac{\underline{\mathbf{W}}_\circ(i,:) \underline{\boldsymbol{\Theta}}_1 \underline{\boldsymbol{\Theta}}_1' \underline{\mathbf{W}}_\circ'(i,:)}{\underline{\mathbf{W}}_\circ(i,:) \underline{\mathbf{H}}(\infty) \underline{\mathbf{W}}_\circ'(i,:)}$$

is maximized (the gain between $\underline{\mathbf{W}}_\circ$ and $\underline{\mathbf{f}}_y(k)$ is an identity matrix, which cannot impose any constraint on $\underline{\mathbf{W}}_\circ$). The designed PRV will have maximized sensitivity to any faults, while having minimum covariance.

Denote $\underline{\mathbf{V}}_\circ \equiv \mathbf{I}_{mp} - \underline{\mathbf{C}}\ \underline{\mathbf{U}}_A\,(\underline{\mathbf{C}}\ \underline{\mathbf{U}}_A)^+$. In line with the work by Frank (1994), we arrive at

$$\begin{aligned}\underline{\mathbf{W}}'_\circ \;=\;& \text{the eigenvectors related to } n_0 \text{ non-zero general eigenvalues of matrix pair} \\ & \{\underline{\mathbf{V}}'_\circ \underline{\mathbf{\Theta}}_1 \underline{\mathbf{\Theta}}'_1 \underline{\mathbf{V}}_\circ, \underline{\mathbf{V}}'_\circ \underline{\mathbf{H}}(\infty) \underline{\mathbf{V}}_\circ\} \end{aligned} \tag{25}$$

Notice that since n_0 is usually much larger than 1, the existence of $\underline{\mathbf{W}}_\circ$ can be guaranteed as analyzed in Li and Shah (2002).

In the absence of faults, $\underline{\mathbf{e}}(k) = \underline{\mathbf{e}}^*(k) \sim \aleph\,[\mathbf{0}, \underline{\mathbf{R}}_e]$. Otherwise, $\underline{\mathbf{e}}(k) \sim \aleph\left[\underline{\mathbf{e}}^f(k), \underline{\mathbf{R}}_e\right]$. Define a scalar $f_D(k) = \underline{\mathbf{e}}'(k)\underline{\mathbf{R}}_e^{-1}\underline{\mathbf{e}}(k)$, which follows a central/non-central chi-square distribution with n_0 degrees of freedom in the normal/faulty case (Johnson and Wincher, 1998). Given a threshold, $\chi^2_\beta(n_0)$, for $f_D(k)$, where β is a level of significance. While $f_D(k) < \chi^2_\beta(n_0)$ indicates the absence of fault, $f_D(k) \geq \chi^2_\beta(n_0)$ triggers fault alarms.

5.3 Fault isolation

To isolate each faulty actuator, sensor, or process component, one needs to transform the PRV into a set of structured residual vectors (SRVs) (Li and Shah, 2002). For simplicity of presentation, first assume that at each time, only a single actuator, sensor, or a process component is faulty. Later the isolation method will be extended to the case where multiple faults occur simultaneously.

5.3.1 Isolation of a single fault

There are l actuators, m sensors and n process components in the system of Eqn. 20. We name a sensor, an actuator, or a process component as an *element*. Similarly to Li and Shah (2002), we design $(l+m+n)$ SRVs, where the i^{th} SRV, $\underline{\mathbf{r}}_i(k)$, is insensitive to a fault in the i^{th} element, but most sensitive to faults in other elements, for $i \in [1, l+m+n]$. The sensitivity/insensitivity of the SRVs to the faulty elements, also termed as *fault isolation logic*, are summarized in Table 1, where a "0"/"1" means the insensitivity/maximized sensitivity of a SRV to a faulty element. In addition, $f^i_u(\ )/f^h_p(\ )/f^j_y(\ )$ stands for the fault in the i^{th} actuator/h^{th} process component/j^{th} sensor, for $i \in [1,l]/h \in [1,n]/j \in [1,m]$.

Denote $\underline{\mathbf{\Theta}}_\circ \equiv \underline{\mathbf{W}}_\circ[\underline{\mathbf{D}}\ |\underline{\mathbf{C}}\ \bar{\underline{\mathbf{B}}}\ |\underline{\mathbf{C}}\ \underline{\mathbf{W}}\ |\ \mathbf{I}_{mp}| - \underline{\mathbf{CL}}] \in \Re^{n_0 \times (2lg+ng+2mp)}$. Mathematically,

SRVs	$f_u^1(\,)$	$\cdots$	$f_u^l(\,)$	$f_p^1(\,)$	$\cdots$	$f_p^n(\,)$	$f_y^1(\,)$	$\cdots$	$f_y^m(\,)$
$\underline{\mathbf{r}}_1(k)$	0	1	$\cdots$	$\cdots$	$\cdots$	$\cdots$	$\vdots$	$\cdots$	$\cdots$
$\vdots$	1	$\ddots$	$\vdots$	$\vdots$	$\vdots$	$\vdots$	$\vdots$	$\vdots$	$\vdots$
$\underline{\mathbf{r}}_l(k)$	$\vdots$	$\ddots$	0	$\vdots$	$\vdots$	$\vdots$	$\vdots$	$\vdots$	$\vdots$
$\underline{\mathbf{r}}_{l+1}(k)$	$\vdots$	$\vdots$	1	0	$\vdots$	$\vdots$	$\vdots$	$\vdots$	$\vdots$
$\vdots$	$\vdots$	$\vdots$	$\vdots$	$\ddots$	$\ddots$	$\vdots$	$\vdots$	$\vdots$	$\vdots$
$\underline{\mathbf{r}}_{l+n}(k)$	$\vdots$	$\vdots$	$\vdots$	$\vdots$	1	0	$\vdots$	$\vdots$	$\vdots$
$r_{l+n+1}(k)$	$\vdots$	$\vdots$	$\vdots$	$\vdots$	$\vdots$	$\ddots$	0	$\vdots$	$\vdots$
$\vdots$	$\vdots$	$\vdots$	$\vdots$	$\vdots$	$\vdots$	$\vdots$	1	$\ddots$	$\vdots$
$\underline{\mathbf{r}}_{l+n+m}(k)$	$\vdots$	$\vdots$	$\vdots$	$\vdots$	$\vdots$	$\vdots$	$\vdots$	$\cdots$	0

Table 1: *Sensitivity and insensitivity of the $l+m+n$ SRVs to faulty elements*

the i^{th} SRV is $\underline{\mathbf{r}}_i(k) = \underline{\mathbf{W}}_i\underline{\mathbf{e}}(k) = \underline{\mathbf{r}}_i^*(k) + \underline{\mathbf{r}}_i^f(k)$, where $\underline{\mathbf{W}}_i$ is a transformation matrix, $\underline{\mathbf{r}}_i^*(k) = \underline{\mathbf{W}}_i\underline{\mathbf{e}}^*(k) \sim \aleph(\mathbf{0}, \underline{\mathbf{R}}_{e,i})$ with $\underline{\mathbf{R}}_{e,i} = \underline{\mathbf{W}}_i\underline{\mathbf{R}}_e\underline{\mathbf{W}}_i'$, and

$$\underline{\mathbf{r}}_i^f(k) = \underline{\mathbf{W}}_i\underline{\mathbf{e}}^f(k) = \underline{\mathbf{W}}_i\underline{\mathbf{\Theta}}_\circ \left[\ \underline{\mathbf{f}}_u'(k)\ \underline{\mathbf{f}}_u'(k-1)\ \underline{\mathbf{f}}_p'(k-1)\ \underline{\mathbf{f}}_y'(k)\ \underline{\mathbf{f}}_y'(k-1)\ \right]'.$$

The fault model for the i^{th} SRV is $\underline{\mathbf{W}}_i\underline{\mathbf{\Theta}}_\circ$. And we split $\underline{\mathbf{\Theta}}_\circ$ into two parts, e.g. $\underline{\mathbf{\Theta}}_\circ = [\underline{\mathbf{\Theta}}_{\circ,i}|\ \underline{\mathbf{\Theta}}_{\circ,i}^\perp]$, where $\underline{\mathbf{\Theta}}_{\circ,i}$ denotes those columns associated with a fault in the i^{th} element, and $\underline{\mathbf{\Theta}}_{\circ,i}^\perp$ the remaining columns.

In the presence of a single sensor fault, $\underline{\mathbf{f}}_u(k)$, $\underline{\mathbf{f}}_u(k-1)$, and $\underline{\mathbf{f}}_p(k-1)$ are zero, but $[\underline{\mathbf{f}}_y'(k)\ \underline{\mathbf{f}}_y'(k-1)]'$ has $2p$ non-zero elements. In this case, $\underline{\mathbf{\Theta}}_{\circ,i}$ has $2p$ columns. If a single actuator fault occurs, $\underline{\mathbf{f}}_y(k) = \mathbf{0}$, $\underline{\mathbf{f}}_y(k-1) = \mathbf{0}$, and $\underline{\mathbf{f}}_p(k-1) = \mathbf{0}$, but $[\underline{\mathbf{f}}_u'(k)\ \underline{\mathbf{f}}_u'(k-1)]'$ has $2g$ non-zero elements. Consequently, $\underline{\mathbf{\Theta}}_{\circ,i}$ has $2g$ columns. Furthermore, in the presence of a single process component fault, i.e. $\underline{\mathbf{f}}_p(k-1) \neq \mathbf{0}$, we can infer that $\underline{\mathbf{\Theta}}_{\circ,i}$ has g columns. We introduce n_{θ_i} to represent the number of independent columns of $\underline{\mathbf{\Theta}}_{\circ,i}$ in each of the three fault cases. Then the maximum value of n_{θ_i} can be $2p$, $2g$, or g.

According to the isolation logic, it is required that $\underline{\mathbf{W}}_i$ is orthogonal to $\underline{\mathbf{\Theta}}_{\circ,i}$ but has maximized covariance with $\underline{\mathbf{\Theta}}_{\circ,i}^\perp$. Denote $\underline{\mathbf{V}}_i \equiv \mathbf{I}_{n_0} - \underline{\mathbf{\Theta}}_{\circ,i}\left(\underline{\mathbf{\Theta}}_{\circ,i}\right)^+$. Using similar algorithms to calculate $\underline{\mathbf{W}}_\circ$, we can obtain the transformation matrices,

$$\underline{\mathbf{W}}_i' \ = \ \text{the eigenvectors related to non-zero general eigenvalues of matrix pair}$$

$$\{\underline{\mathbf{V}}_i'\underline{\mathbf{\Theta}}_{\circ,i}^{\perp}\left(\underline{\mathbf{\Theta}}_{\circ,i}^{\perp}\right)'\underline{\mathbf{V}}_i, \underline{\mathbf{V}}_i'\underline{\mathbf{R}}_e\underline{\mathbf{V}}_i\} \tag{26}$$

$\forall\ i \in [1, l+m+n]$. Note that $\underline{\mathbf{W}}_i$ is $(n_0 - n_{\theta_i}) \times n_0$-dimensional. To assure a non-trivial solution to $\underline{\mathbf{W}}_i$, $n_0 - n_{\theta_i} \geq 1$ must be guaranteed (Li and Shah, 2002).

After fault detection, it follows from the pre-determined isolation logic that

$$\underline{\mathbf{r}}_i(k) \sim \begin{cases} \aleph(\mathbf{0}, \underline{\mathbf{R}}_{e,i}), & \text{if the } i^{th} \text{ element fails;} \\ \aleph(\underline{\mathbf{r}}_i^f(k), \underline{\mathbf{R}}_{e,i}), & \text{if any other element fails;} \end{cases}$$

where $\underline{\mathbf{R}}_{e,i} = \underline{\mathbf{W}}_i\underline{\mathbf{R}}_e\underline{\mathbf{W}}_i'$. Define a scalar fault isolation index $\mathrm{f}_{I,i}(k) = \underline{\mathbf{r}}_i(k)\underline{\mathbf{R}}_{e,i}^{-1}\underline{\mathbf{r}}_i(k)$. If $\mathrm{f}_{I,i}(k)$ follows a chi-square distribution with n_{θ_i} degrees of freedom, but $\mathrm{f}_{I,j}(k)$ does not for $i \in [1, m+l+n]$ and $j \neq i$, then the i^{th} element is faulty. Otherwise, any other but the i^{th} element is faulty. It must be addressed that in compliance with the fault isolation logic presented in Table 1, the i^{th} element corresponds to the i^{th} actuator for $i \in [1, l]$; the $(i-l)^{th}$ process component for $i \in [l, l+n]$; or the $(i-l-n)^{th}$ sensor for $i \in [l+n, l+n+m]$.

5.3.2 Isolation of multiple faults

To isolate multiple faults, one has to use a different isolation logic (Li and Shah, 2002) from the one earlier proposed for a single fault. For the system described by Eqn. 20, any combination of the $m+l+n$ elements can be simultaneously faulty at each time. Theoretically, there are $\sum_{i=1}^{l+n+m} C_i^{l+n+m}$ fault scenarios, where C_i^{l+n+m} denotes the combination of i from $l+n+m$. Note that different fault scenarios occur with different probabilities (Li and Shah, 2002). When one designs an isolation approach, there is no need to consider those scenarios that occur with a very small probability. Instead, only the scenarios that are most likely to occur deserve one's consideration. Therefore, before conducting the design, one has to determine the *maximum number*, f_{max}, of multiple faults, and such a number is usually much smaller than $l+n+m$. This can greatly simplify the design of isolation logic for multiple faults.

For instance, a second order system ($n=2$) with two actuators ($l=2$) and three sensors ($m=3$) has $l+n+m=7$ process elements in total. Suppose that each element has an equal reliability of 95% (In the most general case, each element can have a different and time-varying reliability). Using the formula developed in Li and Shah (2002), we can evaluate

the probabilities, $P_f(q, 95\%, 7, k)$, that $q \in [1, 7]$ elements fail simultaneously. We list them in Table 2. We set up a threshold, e.g. $\epsilon = 4\%$, for $P_f(q, 95\%, 7, k)$. Then only those fault

# of faulty elements: q	1	2	3	4	5	6	7
Probability: $P_f(q, 95\%, 7, k)$	0.2573	0.0406	0.0036	0.0002	0.0000	0.0000	0.0000

Table 2: *Probabilities for* $1 \leq q \leq 7$ *elements to become simultaneously faulty in a system having* 7 *process elements*

scenarios that can occur with a probability higher than this threshold need to be considered. In Table 2, the probability for one or two elements to fail is higher than the threshold, while the probability for three or more elements to simultaneously fail is much smaller than the threshold. Therefore, $f_{max} = 2$ can be determined. Moreover, an isolation logic to isolate one up to two simultaneously faulty elements is chosen and illustrated in Table 3.

	$f_u^1(\ )$	$f_u^2(\ )$	$f_p^1(\ )$	$f_p^2(\ )$	$f_m^1(\ )$	$f_m^2(\ )$	$f_m^3(\ )$
$\underline{\mathbf{r}}_1(k)$	0	0	0	0	1	1	1
$\underline{\mathbf{r}}_2(k)$	1	0	0	0	0	1	1
$\underline{\mathbf{r}}_3(k)$	1	1	0	0	0	0	1
$\underline{\mathbf{r}}_4(k)$	1	1	1	0	0	0	0
$\underline{\mathbf{r}}_5(k)$	0	1	1	1	0	0	0
$\underline{\mathbf{r}}_6(k)$	0	0	1	1	1	0	0
$\underline{\mathbf{r}}_7(k)$	0	0	0	1	1	1	0

Table 3: *Isolation logic for* 1 *up to* 2 *faulty elements in a system having* 7 *elements*

For the seven elements, there are $C_1^7 = 7$ likely scenarios that a single element becomes faulty, and $C_2^7 = 21$ scenarios that two elements become simultaneously faulty. Therefore, in total, there are $7 + 21 = 28$ fault scenarios that need to be uniquely isolated. Based on the isolation logic listed in Table 3, a 7-digit *binary code*, e.g., $J = \underline{\mathbf{r}}_1(k) \times \underline{\mathbf{r}}_2(k) \times \underline{\mathbf{r}}_3(k) \times \underline{\mathbf{r}}_4(k) \times \underline{\mathbf{r}}_5(k) \times \underline{\mathbf{r}}_6(k) \times \underline{\mathbf{r}}_7(k)$, is generated (Qin and Li, 1999; Li and Shah, 2002). And the single faulty sensor can be uniquely isolated using the following logic:

If $J = J_1 = 0\ 1\ 1\ 1\ 0\ 0\ 0$, then the 1^{st} element (the first actuator) is faulty;

$\vdots$

If $J = J_7 = 1\ 1\ 1\ 0\ 0\ 0\ 0$, then the 7^{th} element (the third sensor) is faulty;

because each binary code differs from the others. Secondly, according to the isolation logic, responses of the 7 SRVs to any 2 simultaneously faulty elements, e.g., the i^{th} and the j^{th} elements, $\forall\ \{i, j = [1, 7]\} \cap \{i \neq j\}$, can be described by $J = J_i \vee J_j$, where the $\vee$ stands for binary 'or' operation. Therefore, we can use the following logic to isolate 2 simultaneously faulty sensors

If $J = J_1 \vee J_2 = 0\ 1\ 1\ 1\ 1\ 0\ 0$, then the 1^{st} and 2^{nd} elements are faulty;
$\vdots$
If $J = J_i \vee J_j$, for $i, j = [1, 7], i \neq j$, then the i^{th} and j^{th} elements are faulty.

We obtain 21 unique binary codes, making any combination of 2 simultaneously faulty elements isolable. We summarize the first half of the 28 different binary codes in Table 4 due to limited space.

faulty elements	1	2	3	4	5	6	7	1,2	1,3	1,4	1,5	1,6	1,7	2,3	2,4
$\underline{\mathbf{r}}_1(k)$	0	0	0	0	1	1	1	0	0	0	1	1	1	0	0
$\underline{\mathbf{r}}_2(k)$	1	0	0	0	0	1	1	1	1	1	1	1	1	0	0
$\underline{\mathbf{r}}_3(k)$	1	1	0	0	0	0	1	1	1	1	1	1	1	1	1
$\underline{\mathbf{r}}_4(k)$	1	1	1	0	0	0	0	1	1	1	1	1	1	1	1
$\underline{\mathbf{r}}_5(k)$	0	1	1	1	0	0	0	1	1	1	0	0	0	1	1
$\underline{\mathbf{r}}_6(k)$	0	0	1	1	1	0	0	0	1	1	1	0	0	1	1
$\underline{\mathbf{r}}_7(k)$	0	0	0	1	1	1	0	0	0	1	1	1	0	0	1

Table 4: *Binary codes corresponding to the first* 14 *fault scenarios*

With the chosen isolation logic, seven transformation matrices $\underline{\mathbf{W}}_i$, $\forall\ i = [1, 7]$, can be calculated. Finally, calculating seven SRVs and their associated scalar isolation indices, $\mathrm{f}_{I,i}(k)$, on-line and real-time, one can conduct fault isolation using the similar steps as stated in Section 5.3.1.

5.4 Analysis on fault detectability and isolability

Detectability and isolability of a single fault is analyzed in this subsection. The analysis can also be extended to multiple faults.

5.4.1 Fault detectability conditions

In the PRV, note that

$$\underline{\mathbf{e}}^f(k) = \underline{\mathbf{W}}_\circ[\underline{\mathbf{D}} \ |\underline{\mathbf{C}} \ \underline{\bar{\mathbf{B}}} \ |\underline{\mathbf{C}} \ \underline{\mathbf{W}} \ | \ \mathbf{I}_{mp}| - \underline{\mathbf{C}} \ \underline{\mathbf{L}}] \left[\ \underline{\mathbf{f}}'_u(k) \ \underline{\mathbf{f}}'_u(k-1) \ \underline{\mathbf{f}}'_p(k-1) \ \underline{\mathbf{f}}'_y(k) \ \underline{\mathbf{f}}'_y(k-1) \ \right]'$$

The detectability of a fault is ensured if $\underline{\mathbf{e}}^f(k)$ is always non-zero.

In the presence of a single actuator fault, $\underline{\mathbf{e}}^f(k) = \underline{\mathbf{W}}_\circ[\underline{\mathbf{D}} \ |\underline{\mathbf{C}} \ \underline{\bar{\mathbf{B}}}] \left[\ \underline{\mathbf{f}}'_u(k) \ \underline{\mathbf{f}}'_u(k-1) \ \right]'$. Since $[\underline{\mathbf{f}}'_u(k) \ \underline{\mathbf{f}}'_u(k-1)]'$ has $2g$ non-zero elements, $\underline{\mathbf{e}}^f(k)$ is a linear combination of $2g$ columns of $\underline{\mathbf{W}}_\circ[\underline{\mathbf{D}} \ |\underline{\mathbf{C}} \ \underline{\bar{\mathbf{B}}}]$ specified by the non-zero elements. Apparently, $\underline{\mathbf{e}}^f(k) \neq \mathbf{0}$ requires that the $2g$ columns in $\underline{\mathbf{W}}_\circ[\underline{\mathbf{D}} \ |\underline{\mathbf{C}} \ \underline{\bar{\mathbf{B}}}]$ related to the non-zero elements in $[\underline{\mathbf{f}}'_u(k) \ \underline{\mathbf{f}}'_u(k-1)]'$ are linearly independent.

In the presence of a single process component fault, $\underline{\mathbf{e}}^f(k) = \underline{\mathbf{W}}_\circ \ \underline{\mathbf{C}} \ \underline{\mathbf{W}} \ \underline{\mathbf{f}}_p(k-1)$, where $\underline{\mathbf{f}}_p(k-1)$ has g non-zero elements. It can be similarly understood that fault detectability is guaranteed if the g columns in $\underline{\mathbf{W}}_\circ\underline{\mathbf{C}} \ \underline{\mathbf{W}}$ related to the fault are linearly independent. In the presence of a single sensor fault, $\underline{\mathbf{e}}^f(k) = \underline{\mathbf{W}}_\circ[\ \mathbf{I}_{mp}| - \underline{\mathbf{C}} \ \underline{\mathbf{L}}] \left[\ \underline{\mathbf{f}}'_y(k) \ \underline{\mathbf{f}}'_y(k-1) \ \right]'$. One can assure fault detectability if the $2p$ columns in $\underline{\mathbf{W}}_\circ[\ \mathbf{I}_{mp}| - \underline{\mathbf{C}} \ \underline{\mathbf{L}}]$ associated with the fault are linearly independent.

5.4.2 Fault isolability conditions

Conditions for fault isolability are sensitive to a chosen isolation logic. Herein, we investigate the conditions related to the isolation logic listed in Table 1. To isolate a fault in the i^{th} actuator ($i \in [1, l]$), we should ensure that

$$\underline{\mathbf{r}}^f_i(k) = \underline{\mathbf{W}}_i \ \underline{\mathbf{W}}_\circ[\underline{\mathbf{D}} \ |[\underline{\mathbf{C}} \ \underline{\bar{\mathbf{B}}}] \left[\ \underline{\mathbf{f}}'_u(k) \ \underline{\mathbf{f}}'_u(k-1) \ \right]' = \mathbf{0},$$

but for any $\{j \in [1, l+n+m]\} \bigcap \{j \neq i\}$, $\underline{\mathbf{r}}^f_j(k) = \underline{\mathbf{W}}_j \ \underline{\mathbf{W}}_\circ[\underline{\mathbf{D}} \ |\underline{\mathbf{C}} \ \underline{\bar{\mathbf{B}}}] \left[\ \underline{\mathbf{f}}'_u(k) \ \underline{\mathbf{f}}'_u(k-1) \ \right]' \neq \mathbf{0}$. This requires that the $2g$ columns in $\underline{\mathbf{W}}_j \ \underline{\mathbf{W}}_\circ[\underline{\mathbf{D}} \ |\underline{\mathbf{C}} \ \underline{\bar{\mathbf{B}}}]$ associated with the fault are linearly independent. It can be similarly inferred that to isolate a single component fault, the g columns in $\underline{\mathbf{W}}_j\underline{\mathbf{W}}_\circ\underline{\mathbf{C}} \ \underline{\mathbf{W}}$ associated with the fault must be linearly independent. At last, if the $2p$ columns in $\underline{\mathbf{W}}_j \ \underline{\mathbf{W}}_\circ[\mathbf{I}_{mp}| - \underline{\mathbf{C}} \ \underline{\mathbf{L}}]$ associated with the fault are linearly independent, then a single faulty sensor can be always isolated.

6 A Numerical Example and An Experimental Case Study

In this section, a numerical example and an experimental case study are conducted to test validity of the proposed Kalman filter algorithm in filtering noisy process measurements and the utility of the Kalman filter-based FDI scheme, respectively.

6.1 A numerical example

In this numerical example, the power of the Kalman filter at estimating physical variables from noisy NUSM data is demonstrated. A quadruple tank system(Ge and Fang, 1988) is used as a test bed, which is depicted in Figure 4. In the system, four tanks with the same

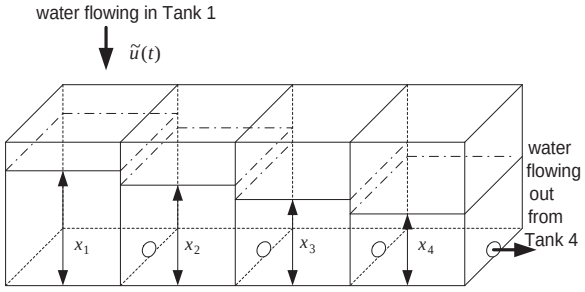

Figure 4: *Schematic of a quadruple tank system*

height and same cross section are serially connected by outlets that have an identical cross section.

Based on the principle of mass balance, the tank system can be modelled by a nonlinear differential equation. After linearizing the equation at a steady operating point, one can describe the tank system (Ge and Fang, 1988) by

$$\dot{\mathbf{x}}(t) = \mathbf{A}\mathbf{x}(t) + \mathbf{B}\tilde{u}(t) + \boldsymbol{\phi}(t),\ \tilde{\mathbf{y}}(t) = \mathbf{C}\mathbf{x}(t)$$

where the input is the water flowing into Tank 1 and simulated by $\tilde{u}(t) = \frac{2500}{9}(1 + 0.36\sin t)$ cm^3 per second. In addition, $\mathbf{x}(t)$ is the state variable vector whose i^{th} element, $x_i(t)$, represents the level of the i^{th} tank physically, for $i \in [1, 4]$; $\tilde{\mathbf{y}}(t)$ is the output vector; and $\boldsymbol{\phi}(t)$ is the process disturbance vector, accounting for the linearization and modelling errors. It is

assumed that $\boldsymbol{\phi}(t)$ is a stationary Gaussian white noise vector with covariance $\mathbf{R}_\phi = 0.1^2\mathbf{I}_4$. Moreover, in the preceding equation, the parameter matrices are

$$\mathbf{A} = \begin{bmatrix} -0.0457 & 0.0457 & 0 & 0 \\ 0.0457 & -0.0914 & 0.0457 & 0 \\ 0 & 0.0457 & -0.0914 & 0.0457 \\ 0 & 0 & 0.0457 & -0.0914 \end{bmatrix}, \ \mathbf{B} = \begin{bmatrix} 0.0020 \\ 0 \\ 0 \\ 0 \end{bmatrix},$$

and $\mathbf{C} = \mathbf{I}_4$.

When one takes samples of $\tilde{\mathbf{y}}(t)$, due to the inevitable measurement noise, one fails to obtain the exact values. However, since the newly developed Kalman filter can estimate the value of $\mathbf{x}(t)$ at different time instants: $t = kT$ from the NUSM data, it turns out from $\tilde{\mathbf{y}}(t) = \mathbf{C}\mathbf{x}(t)$ that the estimate of $\tilde{\mathbf{y}}(k) = \mathbf{C}\mathbf{x}(t)|_{t=kT}$ can be achieved. Especially, if $\mathbf{C}$ is an identity matrix, simply $\tilde{\mathbf{y}}(k) = \mathbf{x}(t)|_{t=kT} = \mathbf{x}(k)$.

Choosing an initial value of the state, $\mathbf{x}(0) = [1\ 1\ 1\ 1]'$, we use the function 'ode45' in MATLAB^{TM} to simulate the tank system, generating the CT signals $\{\tilde{\mathbf{y}}(t), \tilde{u}(t)\}$. Moreover, we select a frame period $T = 0.5$ minute. For $k = [0, 1, \cdots)$, within the period $[kT, kT + T]$, we sample $\tilde{u}(t)$ at $t = kT$ and $t = kT + 0.2$; and $\tilde{\mathbf{y}}(t)$ at $t = kT$ and $t = kT + 0.3$, respectively, obtaining the lifted input and output vectors:

$$\underline{\tilde{u}}(k) = \left[\ \tilde{u}'(kT)\ \tilde{u}'(kT + 0.2)\ \right]' \in \Re^2, \ \underline{\tilde{\mathbf{y}}}(k) = \left[\ \tilde{\mathbf{y}}'(kT)\ \tilde{\mathbf{y}}'(kT + 0.3)\ \right]' \in \Re^8.$$

We introduce Gaussian white noise with covariance $\mathbf{R}_0 = 2^2\mathbf{I}_4$ to the outputs, $\mathbf{y}(\ )$. In addition, we suppose to know $\underline{\tilde{\mathbf{u}}}(k)$. Thus, we have $\underline{\mathbf{y}}(k) = \underline{\tilde{\mathbf{y}}}(k) + \underline{\mathbf{o}}(k)$ and $\underline{\mathbf{u}}(k) = \underline{\tilde{\mathbf{u}}}(k)$.

We generate 1000 samples of lifted data: $\{\underline{\mathbf{u}}(k), \underline{\mathbf{y}}(k)\}$, for $k = 1, 2, \cdots, 1000$, to identify the lifted model of the system, as described by Eqn. 5, including the covariance matrices, $\underline{\mathbf{R}}_\varepsilon$, $\underline{\mathbf{R}}_\omega$ and $\underline{\mathbf{R}}_{\varepsilon,\omega}$. Subsequently, from these identified matrices, we construct the filtering algorithm of the Kalman filter. The system and covariance matrices of the lifted model and the matrices in the filtering algorithm are not reproduced herein due to lack of space.

A set of test data within 2000 frame periods is generated to estimate the state vector $\mathbf{x}(k)$. We present the exact values $\mathbf{x}(k)$ (the first column), the estimated values $\hat{\mathbf{x}}(k|k)$ (the second column), and the errors between the exact and the estimate $\bar{\mathbf{x}}(k|k) = \mathbf{x}(k) - \hat{\mathbf{x}}(k|k)$ (the third column) together in Figure 5. Further, in each column of the figure, the i^{th} subplot

corresponds to i^{th} element of the vector. It must be emphasized that $\hat{\mathbf{x}}(k|k)$ is the optimal estimate of the outputs, $\tilde{\mathbf{y}}(t)$ at $t = kT$, i.e. $\mathbf{y}(k) = \hat{\mathbf{x}}(k|k)$, from the earlier analysis.

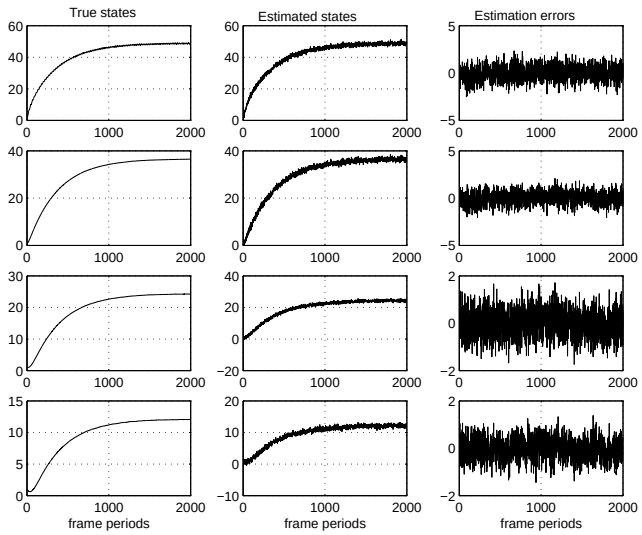

Figure 5: *State estimation results in the numerical example*

We define $r_{n/S} = \sum_{k=1}^{N_0} \|\underline{\mathbf{o}}(k)\| / \|\underline{\tilde{\mathbf{y}}}(k)\|\%$ and $\rho_{\bar{x}/x} = \sum_{k=1}^{N_0} \|\bar{\mathbf{x}}(k|k)\| / \sum_{k=1}^{N_0} \|\mathbf{x}(k)\|\%$ to quantify the noise-to-signal ratio in the lifted output vectors, and state estimation error, respectively. With $N_0 = 2000$, we obtain $r_{n/s} = 14.1\%$ and $\rho_{\bar{x}/x} = 0.52\%$. This indicates that even with pretty high noise-to-signal ratio, the filtering algorithms do give precise estimates of the states.

6.2 The experimental pilot plant

The experimental pilot plant is a continuous stirred tank heater system (CSTHS) located in the Computer Process Control Laboratory, at the University of Alberta. A schematic diagram of the CSTHS is given in Figure 6, where the cold water flowing continuously through the tank is heated by high temperature steam passing through a coil. Four thermocouples, e.g., TT1, TT2, TT3 and TT4, installed at different locations of the long exit pipe provide temperature signals.

The CSTHS system has two inputs ($l = 2$): the cold water and steam flow rates. The inputs are manipulated by respective controllers, and the outputs from the controllers drive

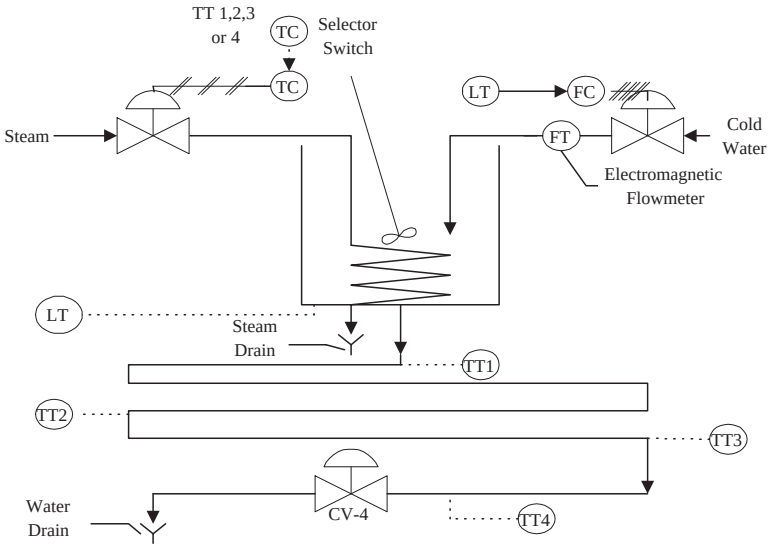

Figure 6: *Schematic diagram of the CSTHS*

the actuators: two valves. We select four variables as the outputs ($m = 4$): the water level in the tank and temperatures $\{\text{TT1}, \text{TT2}, \text{TT3}\}$. Note that TT1 is the temperature of the water in the tank, and TT1 $\neq$ TT2 $\neq$ TT3 due to time delays. The ultimate purpose of the CSTHS is to regulate the outputs.

6.3 Identification of the lifted model of the pilot plant

Select a frame period, $T = 6$ secs. From this pilot plant, a set of training data covering 799 frame periods is collected to identify the lifted model. Within each frame period $[kT, kT+T]$ for $k = 0, 1, \cdots$, the two inputs are sampled at instants kT, $kT+3$, and $kT+4$, while the four outputs are sampled at instants kT and $kT+5$. Thus, the lifted input and output vectors are $\underline{\mathbf{u}}(k) = \left[\begin{array}{ccc} \mathbf{u}'(kT) & \mathbf{u}'(kT+3) & \mathbf{u}'(kT+4) \end{array} \right]' \in \Re^6$, $\underline{\mathbf{y}}(k) = \left[\begin{array}{cc} \mathbf{y}'(kT) & \mathbf{y}'(kT+5) \end{array} \right]' \in \Re^8$, where $g = 3$ and $p = 2$. From $\{\underline{\mathbf{u}}(k), \underline{\mathbf{y}}(k)\}$ for $k = 1, \cdots, 799$, three data matrices, $\underline{\mathbf{U}}_{0,i-1}$, $\underline{\mathbf{Y}}_{0,i-1}$, and $\underline{\mathbf{Y}}_{i,2i-1}$ with $i = 3$, are formed. Subsequently, applying the developed SMI, we estimate, $\underline{\mathbf{A}} \in \Re^{2\times 2}$, $\underline{\mathbf{B}} \in \Re^{2\times 6}$, $\underline{\mathbf{C}} \in \Re^{8\times 2}$, $\underline{\mathbf{D}} \in \Re^{8\times 6}$, $\underline{\mathbf{R}}_{\epsilon} \in \Re^{8\times 8}$, $\underline{\mathbf{R}}_{\omega} \in \Re^{2\times 2}$, and $\underline{\mathbf{R}}_{\omega,\varepsilon} \in \Re^{2\times 8}$.

We use the one step prediction algorithm with a steady Kalman gain combined with $\underline{\mathbf{W}}_{\circ} \in \Re^{6\times 8}$ to generate the PRV for fault detection. For simplicity, only faults in actuators and sensors are considered in this case study. Consequently, six ($l + m = 6$) SRVs for fault

isolation are designed by employing the isolation logic in Table 1. The i^{th} SRV is insensitive to fault in the i^{th} element, but has maximized sensitivity to faults in other elements, for $i \in [1, 6]$. We calculate $\underline{\mathbf{W}}_i \in \Re^{1\times 6}$ and the covariances, $\underline{\mathbf{R}}_e \in \Re^{6\times 6}$ and $\underline{\mathbf{R}}_{e,i} \in \Re^{1\times 1}$, for the PRV and SRVs.

6.4 FDI results

FDI results for only one fault scenario are presented, although we have carried out FDI in many other fault scenarios. Interested readers are encouraged to contact the corresponding author to obtain more details.

An incipient fault simulated by $0.018(t - t_f)$ is introduced to an element at $t_f = 2406$ seconds ($2406/6 = 401$ frame periods). The test data covering 615 frame periods are sampled at the same rate as the training data, and on-line and real-time FDI is carried out. We calculate the fault detection index, $\mathrm{f}_D(k) = \underline{\mathbf{e}}'(k)\underline{\mathbf{R}}_e^{-1}\underline{\mathbf{e}}(k)$, which in the fault-free case, follows a chi-square distribution with degrees of freedom, 6. Therefore, with a pre-selected level of significance $\beta = 0.01$, the confidence limit for $\mathrm{f}_D(k)$ is $\chi^2_{0.01}(6) = 16.812$. We scale $\mathrm{f}_D(k)$ by 16.812 and plot the scaled value, $\bar{f_D}(k) = \mathrm{f}_D(k)/16.812$, in Figure 7. Therein, $\bar{f_D}(k)$ has a unit confidence limit represented by the dashed line in the figure.

We further calculate the fault isolation indices: $f_{I,i}(k)$ for $i \in [1, 6]$ and scale them by their threshold 6.6349. The scaled isolation indices: $\bar{f}_{I,i}(k) = f_{I,i}/6.6349$ are also depicted in Figure 7. It can be seen from the figure that $\bar{f}_D(k)$ is beyond the unit confidence limit after the occurrence of the fault (there is a delay in the detection, because an incipient fault evolves with time slowly). Therefore, fault detection has been successfully performed. Moreover, since $\bar{f}_{I,3}(k)$ is unaffected by the fault (below the unit confidence limit), while $\{\bar{f}_{I,1}(k), \bar{f}_{I,2}(k), \bar{f}_{I,4}(k), \bar{f}_{I,5}(k), \bar{f}_{I,6}(k)\}$ are affected by the fault (beyond the unit limit). The sensitivity of the five fault isolation indices can be characterized by a binary code [1 1 0 1 1 1]. Thus it can be inferred that the third element, which is the first sensor, has a fault.

We define the fault-to-signal ratio as follows to quantify the sensitivity of the proposed FDI scheme, $r_{f/s} = \sum_{k=k_f}^{N_0} \|\underline{\mathbf{f}}_y(k)\| / \sum_{k=k_f}^{N_0} \|\underline{\mathbf{y}}^*(k)\|\%$. In the ratio, k_f is the frame period at which the fault occurs, and N_0 is the number of frame periods in the test data. For the FDI

results displayed in Figure 7, $k_f = 401$, $N_0 = 615$, and $r_{f/s} = 3.74\%$, indicating that the proposed FDI methodology has high sensitivity in detecting and isolating faults.

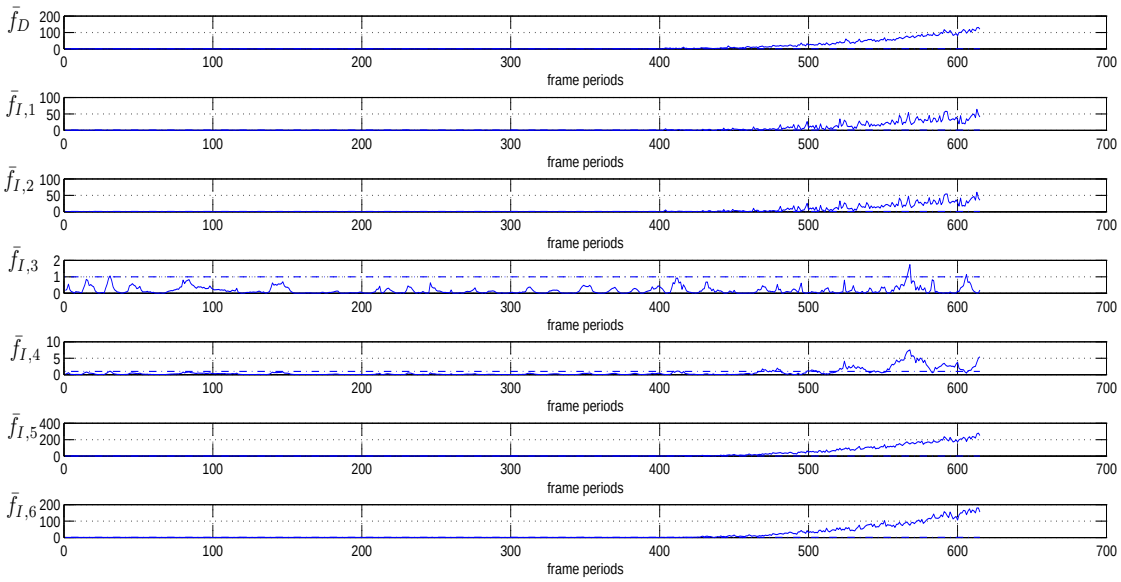

Figure 7: *Detection and isolation of a fault in the* 1^{st} *sensor. The sensitivity of the isolation indices to the fault is* [1 1 0 1 1 1].

7 Conclusion

Data-driven Kalman filters for NUSM systems have been proposed. A numerical example to illustrate estimation of the process variables from a simulated quadruple tank system with NUSM data is provided. Moreover, a novel Kalman filter-based FDI methodology, which gives a unified treatment of faults in actuators, sensors and process components, has been investigated, including analysis on fault detectability and isolability. The developed FDI scheme has been applied to an experimental CSTHS system, where different types of actuator and sensor faults are successfully detected and isolated. The practicality and utility of the proposed theory have been demonstrated.

8 Acknowledgements

Financial aid from the Natural Science and Engineering Research Council (NSERC), Matrikon Inc., and the Alberta Science Research Authority (ASRA) of Canada is gratefully acknowledged.

Appendix, Derivation of Eqn. 4

Multiplying the first line of Eqn. 1 by $\mathbf{e}^{-\mathbf{A}t}$ leads to $\mathbf{e}^{-\mathbf{A}t}\dot{\mathbf{x}}(t) = \mathbf{e}^{-\mathbf{A}t}\mathbf{A}\mathbf{x}(t) + \mathbf{e}^{-\mathbf{A}t}\left[\mathbf{B}\tilde{\mathbf{u}}(t) + \boldsymbol{\phi}(t)\right]$, or equivalently,

$$\frac{d\left[\mathbf{e}^{-\mathbf{A}t}\mathbf{x}(t)\right]}{dt} = \mathbf{e}^{-\mathbf{A}t}\left[\mathbf{B}\tilde{\mathbf{u}}(t) + \boldsymbol{\phi}(t)\right] \tag{27}$$

where $\mathbf{e}^{-\mathbf{A}t}$ is assumed to be non-singular for any t, and $d\left(\mathbf{e}^{-\mathbf{A}t}\mathbf{x}(t)\right)/dt = \mathbf{e}^{-\mathbf{A}t}\dot{\mathbf{x}}(t) - \mathbf{e}^{-\mathbf{A}t}\mathbf{A}\mathbf{x}(t)$.

Integrating Eqn. 27 from $t = kT$ to $t = kT + T$ gives $\mathbf{e}^{-\mathbf{A}(kT+T)}\mathbf{x}(kT+T) - \mathbf{e}^{-\mathbf{A}kT}\mathbf{x}(kT) = \int_{kT}^{kT+T}\mathbf{e}^{-\mathbf{A}t}\left[\mathbf{B}\tilde{\mathbf{u}}(t) + \boldsymbol{\phi}(t)\right]dt$, which can be manipulated into

$$\mathbf{x}(k+1) = \underline{\mathbf{A}}\ \mathbf{x}(k) + \int_{kT}^{kT+T}\mathbf{e}^{\mathbf{A}(kT+T-t)}\left[\mathbf{B}\tilde{\mathbf{u}}(t) + \boldsymbol{\phi}(t)\right]dt, \tag{28}$$

where $\mathbf{x}(k) \equiv \mathbf{x}(kT)$, $\mathbf{x}(k+1) \equiv \mathbf{x}(kT+T)$, and $\underline{\mathbf{A}} \equiv \mathbf{e}^{\mathbf{A}T}$.

With $t \in [kT, kT+T]$, assuming that $\tilde{\mathbf{u}}(t)$ and $\boldsymbol{\phi}(t)$ are *piece-wise constant* within the interval $[kT + t_i^{j-1}, kT + t_i^j]$ for $i \in [1, p]$ and $j \in [1, n_i]$, one can derive

$$\int_{kT}^{kT+T}\mathbf{e}^{-\mathbf{A}t}\mathbf{B}\tilde{\mathbf{u}}(t)dt = \underline{\mathbf{B}}\ \underline{\tilde{\mathbf{u}}}(k), \quad \int_{kT}^{kT+T}\mathbf{e}^{-\mathbf{A}t}\boldsymbol{\phi}(t)dt = \underline{\mathbf{W}}\ \underline{\boldsymbol{\phi}}(k) \tag{29}$$

where, $\underline{\mathbf{B}} = [\underline{\mathbf{B}}_1^1\ \ \cdots\ \underline{\mathbf{B}}_1^{n_1}\ \ \underline{\mathbf{B}}_2^1\ \ \cdots\ \underline{\mathbf{B}}_2^{n_2}\ \cdots\ \underline{\mathbf{B}}_p^1\ \cdots\ \underline{\mathbf{B}}_p^{n_p}] \in \Re^{n\times lg}$, and $\underline{\mathbf{W}} = \underline{\mathbf{B}}|_{\underline{\mathbf{W}}_i^j = \underline{\mathbf{B}}_i^{n_i}} \in \Re^{n\times ng}$.

In Eqn. 29, $\underline{\mathbf{B}}_i^j = \int_{T-t_i^j}^{T-t_i^{j-1}}\mathbf{e}^{\mathbf{A}t}\mathbf{B}dt \in \Re^{n\times l}$ except $\underline{\mathbf{B}}_p^{n_p} = \int_0^{T-t_p^{n_p-1}}\mathbf{e}^{\mathbf{A}t}\mathbf{B}dt$, where $t_i^j = 0$ if $i = 1$ and $j = 0$; $t_i^j = t_{i-1}^{n_{i-1}-1}$ for $i > 1$ and $j = 0$. Using Eqns. 29 in Eqn. 28 gives $\mathbf{x}(k+1) = \underline{\mathbf{A}}\ \mathbf{x}(k) + \underline{\mathbf{B}}\ \underline{\tilde{\mathbf{u}}}(k) + \underline{\mathbf{W}}\ \underline{\boldsymbol{\phi}}(k)$, which is the first line of Eqn. 4.

On the other hand, integrating Eqn. 27 with $t \in [kT, kT+\tau]$ and $0 \le \tau \le T$ produces

$$\mathbf{x}(kT+\tau) \ = \ \mathbf{e}^{\mathbf{A}\tau}\mathbf{x}(k) + \int_{kT}^{kT+\tau}\mathbf{e}^{\mathbf{A}(kT+\tau-t)}\left[\mathbf{B}\tilde{\mathbf{u}}(t) + \boldsymbol{\phi}(t)\right]dt \tag{30}$$

It turns out from the second line of Eqn. 1 that

$$\tilde{\mathbf{y}}(kT+\tau) = \mathbf{C}\mathbf{x}(kT+\tau) + \mathbf{D}\tilde{\mathbf{u}}(kT+\tau) \tag{31}$$

Therefore, the combination of Eqns. 30 and 31 shows

$$\tilde{\mathbf{y}}(kT+\tau) = \mathbf{C}\mathbf{e}^{\mathbf{A}\tau}\mathbf{x}(k) + \mathbf{C}\int_{kT}^{kT+\tau}\mathbf{e}^{\mathbf{A}(kT+\tau-t)}\left[\mathbf{B}\tilde{\mathbf{u}}(t) + \boldsymbol{\phi}(t)\right]dt + \mathbf{D}\tilde{\mathbf{u}}(kT+\tau) \tag{32}$$

For $i \in [1,p]$, evaluating Eqn. 32 at $\tau = t_i$ yields

$$\tilde{\mathbf{y}}(kT+t_i) \;=\; \mathbf{C}_i\mathbf{x}(k) + \mathbf{C}\int_{kT}^{kT+t_i} \mathbf{e}^{\mathbf{A}(kT+t_i-t)}\left[\mathbf{B}\tilde{\mathbf{u}}(t) + \boldsymbol{\phi}(t)\right]dt + \mathbf{D}\tilde{\mathbf{u}}(kT+t_i) \qquad (33)$$

where $\mathbf{C}_i = \mathbf{e}^{\mathbf{A}t_i}$.

For $i \in [1,p]$, when sampling the input and output variables as shown in Figure 1, one can obtain

$$\begin{aligned}
&\tilde{\mathbf{y}}(kT+t_i) = \mathbf{C}_i\mathbf{x}(k) + \\
&[\mathbf{D}_i^1 \;\cdots\; \mathbf{D}_i^i]\left[\; \underline{\tilde{\mathbf{u}}}'(kT+t_1^1)\cdots\underline{\tilde{\mathbf{u}}}'(kT+t_1^{n_1})\cdots\underline{\tilde{\mathbf{u}}}'(kT+t_{i-1}^1)\cdots\underline{\tilde{\mathbf{u}}}'(kT+t_{i-1}^{n_i-1})\;\underline{\tilde{\mathbf{u}}}'(kT+t_i^1)\;\right]' + \\
&[\mathbf{J}_i^1 \;\cdots\; \mathbf{J}_i^i]\left[\; \underline{\boldsymbol{\phi}}'(kT+t_1^1)\cdots\underline{\boldsymbol{\phi}}'(kT+t_1^{n_1})\cdots\underline{\boldsymbol{\phi}}'(kT+t_{i-1}^1)\cdots\underline{\boldsymbol{\phi}}'(kT+t_{i-1}^{n_i-1})\;\underline{\boldsymbol{\phi}}'(kT+t_i^1)\;\right]',
\end{aligned}$$

where, $\mathbf{D}_i^i = \int_0^{t_i-t_{i-1}^{n_{i-1}}} \mathbf{e}^{\mathbf{A}t}\mathbf{B}dt + \mathbf{D}$; $\mathbf{D}_i^j = \mathbf{C}[\int_{t_i-t_{j-1}^{n_{j-1}}}^{t_i-t_j^1} \mathbf{e}^{\mathbf{A}t}\mathbf{B}dt | \int_{t_i-t_j^2}^{t_i-t_j^1} \mathbf{e}^{\mathbf{A}t}\mathbf{B}dt | \cdots | \int_{t-t_j^{n_j}}^{t-t_j^{n_j-1}} \mathbf{e}^{\mathbf{A}t}\mathbf{B}dt] \in \Re^{m\times ln_j}$ and $\mathbf{J}_i^j = \mathbf{D}_i^j|_{\mathbf{B}=\mathbf{I}_n,\mathbf{D}=\mathbf{0}} \in \Re^{m\times nn_j}$ for $j \in [1, i-1]$.

Stacking $\tilde{\mathbf{y}}(kT+t_1)$, $\tilde{\mathbf{y}}(kT+t_2)$, until $\tilde{\mathbf{y}}(kT+t_p)$ together produces the second line of Eqn. 4:

$$\underline{\tilde{\mathbf{y}}}(k) = \underline{\mathbf{C}}\mathbf{x}(k) + \underline{\mathbf{D}}\;\underline{\tilde{\mathbf{u}}}(k) + \underline{\mathbf{J}}\underline{\boldsymbol{\phi}}(k),$$

where

$$\underline{\mathbf{C}} = \begin{bmatrix} \mathbf{C}_1 \\ \mathbf{C}_2 \\ \vdots \\ \mathbf{C}_p \end{bmatrix} \in \Re^{mp\times n} \;,\quad \underline{\mathbf{D}} = \begin{bmatrix} \mathbf{D}_1^1 & \mathbf{0} & \cdots & \cdots & \mathbf{0} \\ \mathbf{D}_2^1 & \mathbf{D}_2^2 & \mathbf{0} & \cdots & \vdots \\ \mathbf{D}_3^1 & \mathbf{D}_3^2 & \mathbf{D}_3^3 & \cdots & \\ \vdots & & & & \vdots \\ \vdots & & & & \mathbf{0} \\ \mathbf{D}_p^1 & \mathbf{D}_p^2 & \mathbf{D}_p^3 & \ldots & \mathbf{D}_p^p \end{bmatrix} \in \Re^{mp\times lg} \text{ with } \mathbf{D}_1^1 = \mathbf{D},$$

and $\underline{\mathbf{J}} = \underline{\mathbf{D}}|_{\mathbf{B}=\mathbf{I}_n,\mathbf{D}=\mathbf{0}} \in \Re^{mp\times ng}$.

References

[1] Aström, K. (1970). *Introduction to stochastic control theory.* New York: Academic Press.

[2] Chen, G., Chen, G., & Hsu, S. (1995). *Linear stochastic control systems.* Florida: CRC Press Inc.

[3] de Souza, C., Gevers, M. & Goodwin, G. (1986). Riccati equations in optimal filtering of nonstabilizable systems having singular state transition matrice. *IEEE Trans. Auto. Cont., 30,* 831-838.

[4] Fadali, M., & Emara-Shabaik, H. (2002). Timely robust detection for multirate linear systems. *International J. of Control*, *75*, 305-313.

[5] Fadali, M., & Liu, W. (1998). Fault detection for systems with multirate sampling. In *Proc. of the American Control Conference*, Philadelphia, PA (pp. 3302-3306).

[6] Frank, P. (1990). Fault diagnosis in dynamic systems using analytical and knowledge-based redundancy – a survey and some new results. *Automatica*, *26*, 459-474.

[7] Frank, P. (1994). Enhancement of robustness in observer-based fault detection. *International J. of Control*, *59*, 955-981.

[8] Ge, W., & Fang, C. (1988). Detection of faulty components via robust observation. *International J. of Control*, *47*, 581-599.

[9] Gudi, R., Shah S.L., & Gray, M. (1994). Adaptive multirate state and parameter estimation strategies with application to a bioreactor. *AIChE J.*, *41*, 2451-2464.

[10] Haykin, S. (1996). *Adaptive filter theory*. New Jersey: Prentice-Hall.

[11] Johnson, R., & Wichern, D. (1998). *Applied multivariate statistical analysis*. New Jersey: Prentice-Hall.

[12] Kalman, R. (1960). A new approach to linear filtering and prediction problems. *Trans. ASME, J. Basic Eng.*, Ser. *82D*, 35-45.

[13] Keller, J. (1999). Fault isolation filter design for linear stochastic systems. *Automatica*, 35, 1701-1706.

[14] Li, W., Han, Z. & Shah, S.L. (2006). Subspace identification for FDI in systems with non-uniformly sampled multirate data. *Automatica*, *42*, 619-627, 2006.

[15] Li, W., Raghavan, H., & Shah, S.L. (2003). Subspace identification of continuous-time residual models for process fault detection and isolation. *J. of Process Control*, *13*, 407-421.

[16] Li, D., Shah, S.L., & Chen, T. (2001). Identification of fast-rate models from multirate data. *International J. of Control*, *74*, 680-689.

[17] Li, W., & Shah, S.L. (2002). Structured residual vector-based approach to sensor fault detection and isolation. *J. of Process Control*, *12*, 429-434.

[18] Li., W. & Shah, S.L. (2004). Fault detection and isolation in non-uniformly sampled systems. In *Proc. of IFAC DYCOPS 7*, Cambridge, MA (6p).

[19] Mehra, R., & Peschon, I. (1971). An innovations approach to fault detection and diagnosis in dynamic systems. *Automatica*, *7*, 637-640.

[20] Moonen, M., DeMoor, B., Vandenberghe, L., & Vandewalle, J. (1989). On and off-line identification of linear state-space models. *International J. of Control*, *49*, 219-232.

[21] Qin, S., & Li, W. (1999). Detection, identification, and reconstruction of faulty sensors with maximized sensitivity. *AIChE J.*, *45*, 1963-1976.

[22] Sheng, J., Chen, T., & Shah, S.L. (2002). Generalized predictive control for non-uniformly sampled systems. *J. of Process Control*, *12*, 875-885.

[23] Sorenson, H. (1970). Least-squares estimation: from Gauss to Kalman. *IEEE Spectrum*, *7*, 63-68.

[24] Sorenson, H. (1985). *Kalman filtering: theory and application* (Ed.). New York: IEEE Press.

[25] Van Overschee, P. & De Moor, B. (1994). N4SID: subspace algorithms for the identification of combined deterministic-stochastic systems. *Automatica*, *30*, 75-93.

[26] Van Overschee, P. & De Moor, B. (1996). *Subspace identification for linear systems-Theory, implementation, applications.* MA: Kluwer Academic Publisher.

[27] Verhaegen, M. (1994). Identification of the deterministic part of MIMO state space models given in innovations form from input-output data. *Automatica*, *30*, 61-74.

[28] Verhaegen, M. & Dewilde, P. (1992). Subspace model identification. part i: the output-error state-space model identification class of algorithms. *International J. of Control*, *56*, 1187-1210.

[29] Verhaegen, M., & Dewilde, P. (1992). Subspace model identification. part ii: analysis of the elementary output-error state-space model identification algorithm. *International J. of Control*, *56*, 1211-1241.

[30] White, J. & Speyer, J. (1987). Detection filter design: spectral theory and algorithms. *IEEE Trans. Auto. Cont.*, *32*, 593-603.

[31] Willsky, A. (1976). A survey of design methods for failure detection in dynamic systems, *Automatica*, *12*, 601-611.

[32] Zhang, P., Ding, S., Wang, G., & Zhou, D. (2002). Fault detection for multirate sample-data systems with time delay. *International J. of Control*, *75*, 1457-1471.